細胞浸潤がみられるようになる。従来，川崎病動脈炎の組織像は，マクロファージ主体の増殖性肉芽腫性炎であるとされてきた。免疫組織学的手法をもちいた近年の検討でも病変局所に出現する炎症細胞の主役が急性期の全経過を通じてCD68陽性マクロファージであることが再確認されたが，さらにこの時期には相当数の好中球も病変局所に出現していることが明らかとなった[4]。炎症はただちに極期に達し，血管壁の全層に波及して汎血管炎と呼ばれる状態になる。このような炎症の極期にあっても多発性動脈炎で認められるようなフィブリノイド壊死はみられない。激しい炎症によって内外弾性板や中膜平滑筋細胞等の動脈壁の既存構築が傷害されると血圧に抗しきれなくなった動脈が拡張をはじめ，風船状拡張と呼ばれる川崎病に特徴的な動脈瘤の形成に至る。動脈瘤は12病日頃に完成するが，動脈瘤の内部では渦流や逆流が発生するため血栓が生じやすく，患児の虚血性心疾患の原因となる（写真）。動脈瘤を作らせないことが川崎病急性期治療の最も重要な点であり，そのためには動脈拡張を引き起こすような激しい汎血管炎に至る前に炎症を消退させる必要がある。以上の病理学的知見は，炎症が極期に至る前の第9病日までに治療が完了されるべきであることを示唆している。

強い炎症細胞浸潤は，25病日頃まで持続するが，その後は徐々に消退することが多く，40病日頃には炎症細胞浸潤はほとんど消失する。全経過を通じて炎症が軽微であった場合には血管炎の瘢痕を残さずに治癒することがあると推測されるが，炎症によって血管壁がある程度破壊された場合には，その瘢痕が残存する。動脈瘤を残した場合には，長期にわたる抗血栓，抗凝固療法を考慮する必要があり，患児の予後に多大な影響を及ぼすこととなる。また，近年では成人期に達する患者数の増加に伴い，血管炎による動脈傷害が後年，粥状動脈硬化症の危険因子となる可能性について議論されるようになってきている。この問題に対するエビデンスはいまだ十分ではなく，今後の検討が待たれる。

川崎病血管炎と炎症性サイトカイン

川崎病では，炎症性サイトカインや接着因子をはじめとする種々の分子異常と冠状動脈炎との関連が報告されている[5]。しかし，これら臨床研究の多くは血清中の各種物質と冠状動脈病変との関連について検討したものであり，血管炎局所における分子異常についての報告は少ない。そこで，代表的な炎症性サイトカインの1つであるtumor necrosis factor α（TNF-α）と転写因子であるnuclear transcription factor κB（NF-κB）について血管炎局所における動態を免疫組織学的に検討してみた。前述のように急性期川崎病血管炎では，マクロファージが浸潤細胞の主体をなすが，これらの多くはNF-κB陽性を呈しており，活性化状態にあると考えられた。さらに，同部ではマクロファージの細胞質内にTNF-α陽性像がみられ，血管炎の成立や維持に活性化マクロファージによるTNF-αの産生が関与している可能性がある。近年，標準的な治療法である免疫グロブリン大量療法に抵抗する症例に対して抗TNF-α療法が試みられるようになってきているが，病理組織学的見地からもこれらが有効な治療戦略となりうる可能性が示唆される。

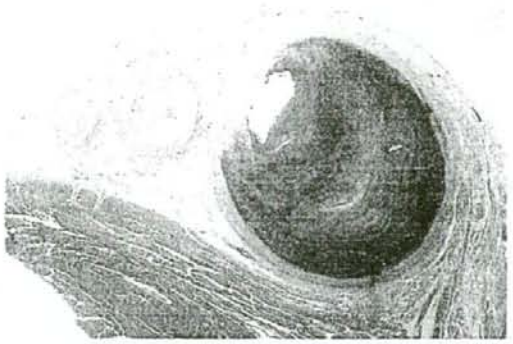

写真　血栓性閉塞をきたした冠状動脈瘤

川崎病血管炎と好中球

川崎病では，動脈炎と活性化好中球の関連や好中球プロテアーゼ阻害薬の有効性についての報告がみられる。血管炎局所においても炎症が極期に達する10病日前後では，マクロファージに混じて多数の好中球が出現していることが明らかとなったが，免疫組織学的にこれらの好中球は，細胞質内に豊富なミエロペルオキシダーゼや好中球エラスターゼを有していた。動脈瘤の完成が12病日頃であることを考慮すると，この時期に好中球から放出される諸因子が動脈壁の破壊に対して大きな役割を演じていることが推察される。

ま と め

急性期川崎病血管炎の病理学的特徴について概説した。従来の形態学的解析や新しい分子生物学的手法によって川崎病血管炎について明らかにされてきた点は多い。しかし，川崎病の原因はいまだ不明である。川崎病急性期における血管傷害についての解析は，新規治療法への示唆を与えるだけでなく，川崎病の原因や病態の解明にも直結する可能性が高い研究領域である。今後は，さらに多分野からの検討とその総合的な解釈が必要と思われる。

文　献

1) 増田弘毅，直江史郎，田中　昇：川崎病（MCLS）における冠状動脈の病理学的検討，特に冠状動脈炎と動脈瘤の形態発生の関連について．脈管学　21：899-912，1981
2) Naoe S, Takahashi K, Masuda H, et al.: Kawasaki disease with particular emphasis on arterial lesions. *Acta Pathol Jpn* 41：785-797, 1991
3) 浅地　聡，増田弘毅，田中　昇，ほか：川崎病における腎病変の病理形態学的研究．冠状動脈病変との関連も考慮して．脈管学　29：453-460，1989
4) Takahashi K, Oharaseki T, Naoe S, et al.: Neutrophilic involvement in the damage to coronary arteries in acute stage of Kawasaki disease. *Pediatr Int* 47：305-310, 2005
5) 佐地　勉，監物　靖，高月晋一，ほか：川崎病の血管病変．リウマチ科　34：64-73，2005

好中球機能異常による呼吸器不全
——ミエロペルオキシダーゼ欠損を中心に

荒谷康昭
横浜市立大学大学院国際総合科学研究科 理学・バイオ科学専攻

好中球は感染局所から産生されるサイトカイン・ケモカインに応答して感染部位に遊走し，感染の初期防御に働く．病原体を貪食した好中球は，食細胞NADPH オキシダーゼによりスーパーオキシド($O_2^{\cdot-}$)を産生し，$O_2^{\cdot-}$からは非酵素的に過酸化水素(H_2O_2)がつくられる．さらに，ミエロペルオキシダーゼ(MPO)の触媒によって，H_2O_2と塩素イオン(Cl^-)から次亜塩素酸(HOCl)が産生する(図 1)．MPO は好中球のみに存在しており，単球内でもわずかに検出されるほかにはMPO を発現している組織は同定されていない．このように，好中球は種々の活性酸素種を積極的に産生する能力が発達している[1]．

食細胞 NADPH オキシダーゼに遺伝的変異があると，正常な細胞内殺菌ができず，重症感染を繰り返す慢性肉芽腫症(chronic granulomatous disease：CGD)を発症する．NADPH オキシダーゼ($gp91^{phox}$)欠損マウスもアスペルギルス感染によって重篤な呼吸器不全を発症する[2]．一方，わが国では 1/57,000 の頻度とされる MPO 欠損症[3]の臨床症状はカンジダ易感染傾向にある．MPO 欠損好中球は乳酸菌，黄色ブドウ球菌，カンジダ真菌などの細菌や真菌に対する殺菌作用が弱く，また，この酵素はインフルエンザウイルス[4]やヒト免疫不全ウイルスなどの殺ウイルス作用にも働いている．

著者らが作製した MPO ノックアウトマウス(MPO-KO マウス)にカンジダ(*C. albicans*)を経鼻的に肺感染させたところ，野生型マウスはまったく死亡しない菌量でも，MPO-KO マウスは重度の肺炎を発症して顕著な生存率の低下を示し，5 日目までにはそのほとんどが死亡した．MPO-KO マウス肺では経時的残存菌数がほとんど低下しなかったことが肺炎重篤化の原因と考えられた[5]．さらに，カンジダに限らず，アスペルギルスやトリコスポロンなどの真菌や，緑膿菌やクレブシエラなどの細菌を肺感染させても，感染 2 日目の比較において MPO-KO マウスは野生型マウスに比べて有意な易感染性を示した[6]．MPO-KO マウスと CGD マウスの腹腔にカンジダを接種して病態を比較したところ，接種量が低量であれば CGD マウスのほうが重篤な症状を示したが，高量になるにつれて，MPO-KO マウスは CGD マウスに匹敵する病態を示した[7]．したがって，MPO 欠損者が多量のカンジダ菌に感染すると，CGD 患者と同程度の深刻な感染症を患う危険性があると推察される．

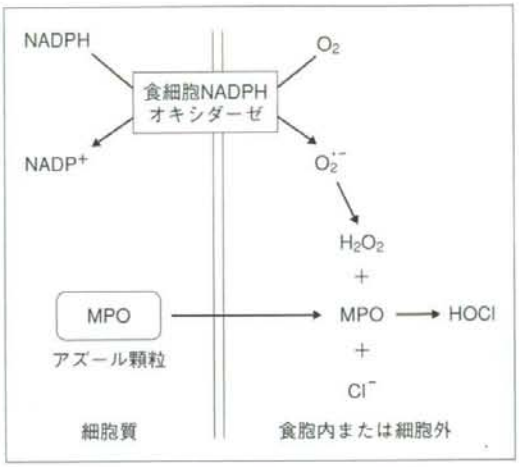

図 1　好中球が産生する活性酸素[1]

クリプトコッカスを肺感染後 20 日頃までの病態は，野生型と MPO-KO マウスとで差は認められなかった．したがって，MPO 欠損という好中球機能異常は本菌に対する初期生体防御には影響しないと考えられる．ところが，1 カ月経過後の MPO-KO マウス肺での残存菌数は野生型よりも顕著に多く，野生型マウスよりも重篤な肺炎像を示し(図 2)，生存率は徐々に低下しはじめ，2 カ月経過後にはほとんどすべてが死亡した．感染 7 日目の MPO-KO マウス肺のサイトカイン量を野生型マウスと比較したところ，IL-4 が有意に高く，IL-2, IL-12p70, IFN-γ は逆に低値を示した[8]．クリプトコッカスの感染防御には Th1 依存性の免疫応答がおもな役割を担っているので，MPO の欠損によって Th1 応答が鈍化していることが易感染性の一因であると考えられる．

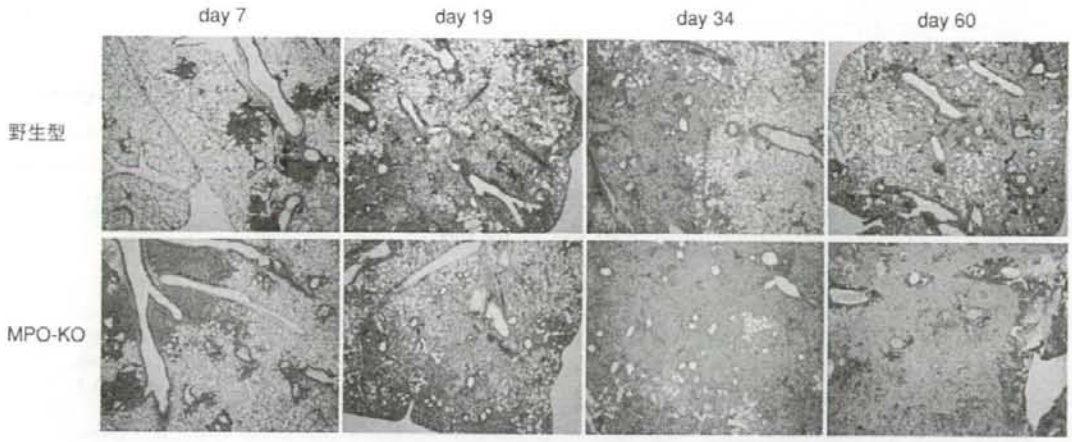

図 2　クリプトコッカス(*C. neoformans*)を経鼻感染後の肺のHE染色像[8]

MPO は多種の真菌や細菌感染に対する生体防御に直接的に機能しているだけでなく，自然免疫系と細胞性免疫系とのクロストークにもかかわっているのかもしれない．

1) Klebanoff, S. J. : *J. Leukoc. Biol.*, **77** : 598-625, 2005.
2) Pollock, J. D. et al. : *Nat. Genet.*, **9** : 202-209, 1995.
3) Nunoi, H. et al. : *Microbiol. Immunol.*, **47** : 527-531, 2003.
4) Yamamoto, K. et al. : *J. Infect. Dis.*, **164** : 8-14, 1991.
5) Aratani, Y. et al. : *Infect. Immun.*, **67** : 1828-1836, 1999.
6) Aratani, Y. et al. : *J. Infect. Dis.*, **182** : 1276-1279, 2000.
7) Aratani, Y. et al. : *J. Infect. Dis.*, **185** : 1833-1837, 2002.
8) Aratani, Y. et al. : *J. Med. Microbiol.*, **55** : 1291-1299, 2006.

*　　*　　*

【真菌・細菌感染防御の鍵：好中球Myeloperoxidase】

Role of myeloperoxidase for the host defense against bacterial and fungal infection

荒谷　康昭

Aratani　Yasuaki

Key words
好中球，ミエロペルオキシダーゼ，
活性酸素，感染防御，
ノックアウトマウス

要　約

自然免疫系の一員である好中球は，さまざまな活性酸素を産生して，感染防御の最前線を担っている。ミエロペルオキシダーゼ（MPO）は，主として好中球に存在しており，H_2O_2とCl^-からOCl^-が産生される反応を触媒する。この酵素の感染防御における重要性については，1970年頃から精力的に研究が進められてきたが，個体レベルでの重要性が明らかにされ始めたのはごく最近のことである。本稿では，MPOのノックアウト（MPO-KO)マウスを用いた研究成果を中心に，真菌・細菌に対する感染防御における*in vivo*でのMPOの役割について概説する。

はじめに

病原微生物の感染などで活性化した好中球は，まず食細胞NADPHオキシダーゼにより，酸素からスーパーオキシド（O_2^-）を産生する。次いで非酵素的に，あるいはスーパーオキシドディスムターゼの触媒によって，O_2^-から過酸化水素（H_2O_2)ができ，鉄イオンの存在下でH_2O_2から・OHが生成する。さらに，アズール顆粒内に貯蔵されていたMPOが食胞内あるいは細胞外に放出され，この酵素の触媒によってH_2O_2とCl^-からHOClが生成する。このように，活性化した好中球は，O_2^-を基にして，さまざまな活性酸素を産生し放出する。活性酸素は，生体内のすべての細胞においてわずかながら常につくられているが，そのほとんどは，電子伝達系の漏れとして生じているものである。それに対して，好中球はむしろ積極的に活性酸素を産生する細胞である。

ミエロペルオキシダーゼ（MPO)は，59 kDaの重鎖と14 kDaの軽鎖が2本ずつ会合したヘテロテトラマーであり，2分子のヘムをもつ。骨髄における顆粒球分化の過程で，前骨髄球と前骨髄単球だけがMPOを発現する。したがって、成熟好中球では，MPO蛋白質はアズール顆粒内に大量に貯蔵されているが，その遺伝子発現は停止している。血液中の単球にもこの酵素がわずかに存在しているが、その他の組織や細胞には存在しない[1]。MPO欠損症の頻度は比較的高く，米国やヨーロッパでは2,000～4,000人に1人，我が国では57,135人に1人[2]とされている。その原因となるアミノ酸置換として，R569W，Y173C，M251T，G501S, R299Cなどが知られている。MPO活性を欠如しているにもかかわらず健康な例も少なくないが，糖尿病などを患っているMPO欠損患者は，予後の悪いカンジダ症をしばしば発症するので，臨床的に問題となる。

1．感染防御におけるMPOの重要性

真菌・細菌感染防御におけるMPOの役割に関する研究は，1970年頃のKlebanoffやLehrerらの研究に始まる。彼らは，血液から単離した好中球の試験管内での殺菌力を調べた。その結果，ペルオキシダーゼ阻害剤存在下の好中球や，MPO欠損者から単離した

横浜市立大学大学院国際総合科学研究科　理学バイオ科学専攻
：International Graduate School of Arts and Sciences Yokohama City University
〒236-0027　横浜市金沢区瀬戸22-2　　e-mail：yaratani@yokohama-cu.ac.jp

表1　野生型マウスとMPO-KOマウスの肺における殺菌能の比較
（文献7を改変）

病原体	肺あたりの菌数（対数値）			48時間後のMPO-KO肺の菌数 / 48時間後の野生型肺の菌数
	感染させた菌数	感染後48時間		
		野生型	MPO-KO	
Candida albicans	6.71	4.83 ± 0.20	6.31 ± 0.16	30.2
	5.71	3.56 ± 0.16	5.38 ± 0.14	66.1
Candida tropicalis	6.00	4.12 ± 0.17	5.64 ± 0.13	33.1
	5.14	3.04 ± 0.24	3.51 ± 0.14	3.0
Trichosporon asahii	5.96	4.66 ± 0.08	6.08 ± 0.13	26.3
	5.11	3.57 ± 0.18	4.16 ± 0.07	3.9
Aspergillus fumigatus	5.68	2.19 ± 0.18	3.55 ± 0.24	22.9
	5.22	1.75 ± 0.50	2.86 ± 0.22	12.9
Cryptococcus neoformans	6.80	7.70 ± 0.27	7.73 ± 0.22	1.1
	4.68	5.67 ± 0.09	5.50 ± 0.22	0.7
Pseudomonas aeruginosa	5.83	3.52 ± 0.26	6.26 ± 0.31	550.0
	4.97	2.78 ± 0.10	2.90 ± 0.18	1.3
Klebsiella pneumoniae	6.78	3.34 ± 0.26	4.31 ± 0.31	9.3
	5.22	<1.0	1.91 ± 0.85	>8.1
Staphylococcus aureus	8.16	3.76 ± 0.15	4.56 ± 0.49	6.3
	7.02	2.05 ± 0.49	2.00 ± 0.30	0.9
	6.13	1.55 ± 0.13	1.89 ± 0.16	2.2
Streptococcus pneumoniae	7.37	4.57 ± 0.72	4.17 ± 0.55	0.4
	6.06	2.71 ± 0.85	3.14 ± 1.76	2.7

好中球は，乳酸菌，ブドウ球菌，カンジダ真菌を殺菌する能力が正常好中球よりも弱いことや[3]，糖尿病を患っているMPO欠損者の好中球では，カンジダ殺菌能がさらに低下していることなどが明らかとなり[4]，感染防御におけるMPOの重要性が初めて示された。その後，MPOがインフルエンザウイルス[5]やヒト免疫不全ウイルスなどの殺ウイルス作用にも働いていることも報告された。

筆者らは，MPOのノックアウトマウス（MPO-KOマウス）を作製して，このマウスの生体防御能を調べ，個体レベルでのMPOの重要性を初めて示した[6]。このマウスの好中球は，HOCl産生能のみが特異的に欠如しており，O_2^-産生量は正常である。まず，このマウスにカンジダ菌（*Candida albicans*）を経鼻的に肺感染させると，わずか5日の間におよそ7割のマウスが死亡した。また，野生型マウスの肺における残存菌数は経時的に速やかに減少したのに対し，MPO-KOマウスの肺の菌数はほとんど減少しなかった。その結果，MPO-KOマウスは重度の肺炎を発症し，これが原因で死亡したと考えられる。すなわち，カンジダ菌の肺感染に対する初期の生体防御にMPOが極めて重要であることが，個体レベルで証明された。

次に，その他の真菌や細菌に対する初期感染防御におけるMPOの重要性を知るために，各種真菌・細菌を肺感染させた48時間後の肺中の残存菌数を，野生型マウスとMPO-KOマウスとで比較した（表1）[7]。その結果，MPO-KOマウスは，アスペルギルス（*Aspergillus fumigatus*）やトリコスポロン

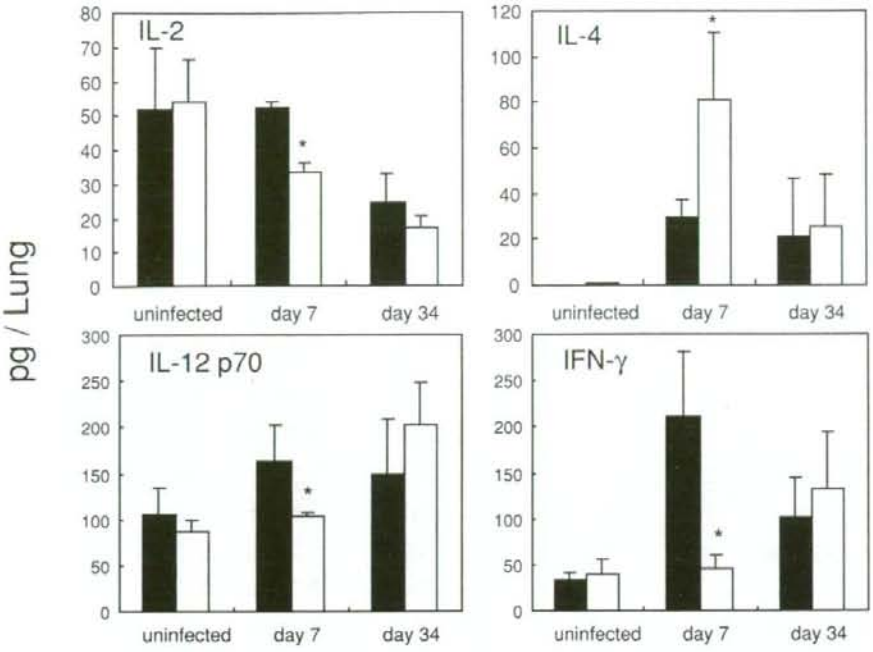

図1　クリプトコッカス（*C. neoformans*）を経鼻感染後，7日目と34日目の肺でのサイトカイン量
野生型マウス（■）とMPO-KOマウス（□）にクリプトコッカス（*C. neoformans*）を経鼻的に肺感染させ，図示した日数において，肺ホモジネート上清のサイトカイン量を測定した。*, $P < 0.05$（文献8を改変）

（*Trichosporon asahii*）などの真菌と，緑膿菌（*Pseudomonas aeruginosa*）やクレブシエラ（*Klebsiella pneumoniae*）などの細菌に対して，著しい殺菌能の低下が認められた。一方，黄色ブドウ球菌（*Staphylococcus aureus*）と肺炎球菌（*Streptococcus pneumoniae*）の殺菌力の低下はほとんど認められなかった。このことから，MPOは多種の真菌や細菌感染に対する生体防御にきわめて重要な酵素であることがわかる。しかも、この酵素は，細菌よりも真菌に対する生体防御に，より強くはたらいているようである。

2. 自然免疫と細胞性免疫のクロストークにおけるMPOの関与

さて，クリプトコッカス（*Cryptococcus neoformans*）を肺感染させ，上記と同様に48時間後の残存菌数を比較したところ，野生型とMPO-KOマウスとでまったく差は認められなかった（表1）。ところが，おもしろいことに，感染7日目頃から菌数の差が生じ始め，1ヶ月後のMPO-KOマウスでは，野生型マウスよりもおよそ100倍の菌が残存した。さらに，MPO-KOマウスは，1ヶ月後から肺炎が徐々に重篤化し，その結果，最初の1ヶ月は全く死亡しなかったにもかかわらず，1ヶ月後から徐々に死亡し始め，2ヶ月経過後にほとんどすべてが死亡した。すなわち，好中球由来のHOClは，クリプトコッカスに対する生体防御にも重要な役割を担っていることがわかった。しかし，感染48時間後の感染初期におけるMPO-KOマウスの感染防御能は野生型マウスと差がなかったことや，クリプトコッカスの感染防御にはTh1依存性の細胞性免疫応答が最重要であるという従来の知見を考え合わせると，HOClがクリプトコッカスを直接的に殺菌しているとは考えにくい。

そこで，感染7日目のMPO-KOマウス肺のサイトカイン量を野生型マウスと比較したところ，IL-2，IL-12p70，IFN-γは有意に低く，IL-4は逆に高値を示した（図2）[8]。この結果は，MPOの欠損がTh1依存性の細胞性免疫応答を鈍化させたことにより，クリプトコッカスに対する防御能が低下した可能性を

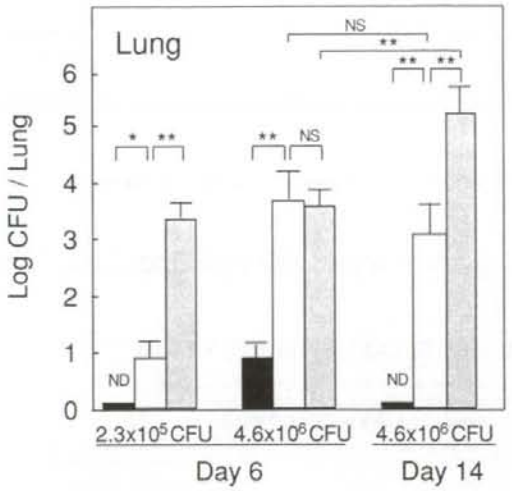

図2　カンジダ菌（*C. albicans*）を感染後，6日目と14日目に肺で検出された菌数
野生型（■），MPO-KO（□），CGD（▥）の各マウスに図示した菌数を腹腔に接種した。ND，検出限界（10 CFU）以下; NS, 有意差なし；*P < 0.05; **P < 0.01（文献10を改変）

示唆している。MPOはHOClを産生して，多種の真菌や細菌を直接的に殺菌しているだけでなく，細胞性免疫系の賦活化にも働いているのかも知れない。

3. MPO欠損と食細胞NADPHオキシダーゼ欠損の比較

食細胞NADPHオキシダーゼ（Nox2)の欠損患者は慢性肉芽腫症を発症し，幼少期から重篤な感染を頻発する。また，この酵素のノックアウトマウス（CGDマウス）は，アスペルギルスや黄色ブドウ球菌などに易感染性を示す[9]。野生型，MPO-KO，CGDの各マウスに，低量（2.3 x 10^5 CFU），中量（4.6 x 10^6 CFU），高量（6.9 x 10^7 CFU）のカンジダ菌を感染させて生存率を比較したところ，野生型マウスは高量の菌を接種してもほとんど死亡しなかったが，CGDマウスの生存率は，予想どおり菌量依存的に低下した。さて，興味深いことに，MPO-KOマウスは，低量感染では野生型マウスと同程度の生存率であったが，高量を感染させるとCGDマウスと同程度の顕著な生存率の低下を示した。感染6日目と14日目の肺の菌数を測定した（図2）[10]。CGDマウスの感染重篤度は接種した菌量依存的に増大したが，野生型マウスの感染は中量の菌を接種してもごく軽度であった。興味深いことに，MPO-KOマウスでは，中量の菌を接種するとCGDマウスに匹敵する重篤な感染を示したが，低量では野生型マウスと同程度の極めて軽度な感染しか示さなかった。また，中量の菌を接種した際，6日目のMPO-KOマウス肺の菌数はCGDと同程度だったが，14日目ではCGDマウスよりも著しく減少した。すなわち，MPOは多量の菌が感染したときの初期生体防御機構として，食細胞NADPHオキシダーゼに匹敵する重要な役割を担っていることがわかった。

おわりに

真菌・細菌感染に対する防御系としてのMPO/H2O2/Cl^-系の，個体レベルでの重要性を紹介した。しかし，好中球が感染防御のために産生するHOClやその代謝産物は，殺菌力が強い反面，宿主の組織にも直接的あるいは間接的に傷害を及ぼすと考えられる。事実，MPO活性と癌，腎障害，動脈硬化，アルツハイマー発症との相関性が示唆されている。また，一方では，MPO抗体（ANCA）と血管炎との関連も明らかにされようとしている（長尾，鈴木の項参照）。このように，MPOあるいは好中球由来の活性酸素が関与するさまざま病態が，次々と解明されようとしている。

文　献

1) Klebanoff, SJ: Myeloperoxidase: J Leukoc Biol 77 : 598-625, 2005.
2) Nunoi H, Kohi F, Kajiwara H, Suzuki K : Microbiol. Immunol 47 : 527-531, 2003.
3) Klebanoff SJ: Science. 169 :1095-1097, 1970.
4) Lehrer, R. I. and M. J. Cline: J Clin Invest. 48 : 1478-1488, 1969.
5) Yamamoto K, Miyoshi-Koshio T, Utsuki Y, *et al.* : J Infect Dis. 164 : 8-14, 1991.
6) Aratani Y, Koyama H, Nyui S, *et al.*: Infect Immun 67 : 1828-1836, 1999.
7) Aratani Y, Kura F., Watanabe H., *et al.*: J Infect Dis 182 : 1276-1279, 2000.
8) Aratani, Y., Kura, F., Watanabe, H., *et al.*: J Med Microbiol. 55 : 1291-1299, 2006.
9) Pollock JD, Williams DA, Gifford MA, *et al.*: Nat Genet 9 : 202-209, 1995.
10) Aratani Y, Kura F, Watanabe H, *et al.*: J Infect Dis 185 : 1833-1837, 2002.

Journal of Neuroimmunology xxx (2008) xxx–xxx

Contents lists available at ScienceDirect

Journal of Neuroimmunology

journal homepage: www.elsevier.com/locate/jneuroim

The effects of MPTP on the activation of microglia/astrocytes and cytokine/chemokine levels in different mice strains

Y. Yasuda [a,*], T. Shimoda [a,b], K. Uno [a], N. Tateishi [a,b], S. Furuya [a], K. Yagi [a], K. Suzuki [c], S. Fujita [a]

[a] Cell Biology Section, Division of Basic Research, Louis Pasteur Center for Medical Research, 103-5, Sakyo-ku, Tanaka, Monzen-cho, Kyoto 606-8225, Japan
[b] Serpha Medical Research Institute Co., Ltd., Kobe Univ. Incubation Center 402, 1-5-1 Minatojima-minami-machi, Chuo-ku, Kobe 650-0047, Japan
[c] Department of Immunology, Inflammation Program, Chiba University Graduate School of Medicine, Inohana 1-8-1, Chuo-ku, Chiba, 260-8670, Japan

ARTICLE INFO

Article history:
Received 13 May 2008
Received in revised form 6 August 2008
Accepted 11 August 2008
Available online xxxx

Keywords:
MPTP sensitivity
Mice
Strain difference
Cytokine
Chemokine
Glia

ABSTRACT

The effects of MPTP on two mouse strains with different MPTP sensitivities and immunological backgrounds were compared: MPTP-sensitive C57BL/6 mice (B6) with a propensity for Th1 and less MPTP-sensitive BALB/c mice (BALB) with a propensity for Th2. It was found that acute MPTP treatment induced behavioral dysfunction, activated microglia/astrocytes, and increased the levels of IL-10, IL-12(p40) IL-13, IFN-γ, and MCP-1 in CSF in B6, but not in BALB. This suggests that variances in immunological backgrounds might be a major contributing factor in sensitivity differences to MPTP.

1. Introduction

Parkinson's disease (PD) is an age-related, neuro-degenerative disease characterized by bradykinesis, postural instability, and gait disturbance due to a loss of dopamine (DA) neurons in the substantia nigra *pars compacta* (SNpc). Methyl-4-phenyl-1,2,3,6-tetrahydropyridine (MPTP) is known to specifically affect DA neurons in the SNpc of animals. MPTP is converted into MPP^+ (mitochondrial toxin) in astrocytes of the striatum and accumulates selectively in the striatal dopaminergic nerve fibers via uptake through the high affinity dopamine transporter (DAT) (Bezard et al., 1999; Chiba et al., 1985), specifically inducing the death of DA neurons and resulting in the development of PD-like symptoms in several kinds of mammals, including humans, non-human primates and mice (Przedborski et al., 2001). Mice, however, show strain differences in sensitivity to MPTP. MPTP acute treatment, devised in order to study acute phases of PD, induces more severe transient movement dysfunction and DA neuron loss in C57BL/6 (B6), as compared to BALB/c (BALB) (Sedelis et al., 2000). Degradation of the nerve endings of DA neurons in the striatum precedes degeneration in the cell bodies of DA neurons in SNpc (Jackson-Lewis et al., 1995). Therefore, events occurring in the striatum, especially in the MPTP model, are thought to be representative of the early stages of pathological mechanisms involved in the degenerative processes.

Inflammatory processes play a vital role in the etiological mechanisms that lead to PD (Barcia et al., 2003; Carvey et al., 2005; Hunot and Hirsch, 2003; Liu, 2006; Nagatsu and Sawada, 2005; Sawada et al., 2006).

A major player in brain inflammation, related to PD pathogenesis, is thought to be microglia (Kim and Joh, 2006). It has been reported that astocytes are also involved in brain inflammation, in addition to microglia (Carpentier et al., 2005). Both types of brain immune cells, microglia and astrocytes, are activated during the process of DA neuron loss (Hirsch et al., 1999), suggesting that activation of microglia/astrocytes might be related to PD pathogenesis. Inhibition of microglial activation attenuates the loss of DA neurons in experimental models (Du et al., 2001; Wu et al., 2002). Some non-steroidal anti-inflammatory drugs (NSAIDs) reduce the incidences of PD in humans (Chen et al., 2003; Wahner et al., 2007). Inflammatory-related changes of cytokine (interleukin-1α (IL-1α), IL-1β, IL-6, interferon-γ (INF-γ), tumor necrosis factor-α (TNF-α)) and chemokine (monocyte chemotactic protein-1 (MCP-1), macrophage inflammatory protein-1α (MIP-1α), and MIP-1β) expression in PD patients as well as in PD model animals have been reported (Hunot and Hirsch, 2003; Kalkonde et al., 2007; Kim and Joh, 2006; Nagatsu and Sawada, 2005; Pattarini et al., 2007). Although the role of astrocytes in PD pathogenesis and progression remains unclear, there is enough evidence to suggest that neuroinflammation and activated microglia contribute to DA neuronal death resulting in PD (Hunot and Hirsch, 2003; Kim and Joh, 2006; Nagatsu and Sawada, 2005; Sawada et al., 2006; Teismann and Schulz, 2004).

Highly MPTP-sensitive B6 and less MPTP-sensitive BALB have different immunological backgrounds. In acquired immune responses,

* Corresponding author. Tel.: +81 75 791 7726; fax: +81 712 5850.
E-mail address: yyasuda@louis-pasteur.or.jp (Y. Yasuda).

0165-5728/$ – see front matter © 2008 Elsevier B.V. All rights reserved.
doi:10.1016/j.jneuroim.2008.08.003

Please cite this article as: Yasuda, Y., et al., The effects of MPTP on the activation of microglia/astrocytes and cytokine/chemokine levels in different mice strains, J. Neuroimmunol. (2008), doi:10.1016/j.jneuroim.2008.08.003

the balance between two subsets of helper T cells (Th), that is, type 1 helper T cell (Th1)/type 2 helper T cell (Th2) is important. Th1 and Th2 are characterized by their distinct cytokine profiles (Mosmann and Sad, 1996). IL-2, IFN-γ and TNF-α are Th1 cytokines and IL-4, IL-5, IL-6, IL-10 and IL-13 are Th2 cytokines. Activation of Th1 promotes cell-mediated immunity and activation of Th2 promotes humoral immunity. B6 and BALB show a bias toward Th1 and Th2, respectively (Heinzel et al., 1989). Therefore, a comparative study of B6 and BALB, in terms of their MPTP-sensitivity and MPTP effects on cytokine/chemokine production, might be helpful in revealing the role of immune responses in PD pathogenesis.

In order to clarify whether immunological variance causes strain dependent differential sensitivity towards MPTP in mice, we have performed a comparative study between B6 and BALB, specifically focusing on the degree of movement dysfunction, activation of microglia/astrocytes in the striatum, and alterations of cytokine/chemokine levels in cerebrospinal fluid (CSF) and plasma after MPTP acute treatment. Activation of microglia/astrocytes was studied immuno-histochemically using an antibody against a microglial marker protein, ionized calcium binding adaptor molecule 1 (Iba1) (Yasuda et al., 2007), and an astrocyte marker protein, S100B. Twenty-three kinds of cytokine/chemokine were simultaneously measured by multiplexed fluorescent bead-based immunoassay to determine the mutual relationship of cytokines/chemokines following PD pathogenesis.

2. Materials and methods

2.1. Animals and MPTP treatment

Male B6 and BALB (7 weeks old) were purchased from Japan SLC (Hamamatsu, Japan) and housed in a temperature-controlled room for 7 days prior to MPTP-injection. All experiments were conducted in accordance with the Guidelines on Experimental Animals compiled by the Animal Care and Animal Use Ethical Committee; Louis Pasteur Center for Medical Research.

MPTP (Sigma-Aldrich, St. Louis, MO, USA) was dissolved in saline and 20 mg/kg body weight was injected intraperitoneally in mice 4 times at 2-hour intervals (Yasuda et al., 2007).

Mice were deeply anesthetized with sodium pentobarbital at −3 (1 h after the second MPTP injection), −1 (1 h after the third MPTP injection), 1, 3, 6, 12 h and days 1, 2 and 3 after MPTP treatment (Fig. 1). After the collection of their CSF and plasma, mice were perfusion-fixed with 4% paraformaldehyde in a 0.1 M phosphate buffer (PB; pH7.2) following a heparinized saline perfusion. Brains were post-fixed in the same solution for 1 h, infiltrated with 15% sucrose overnight and kept at −80 °C until use.

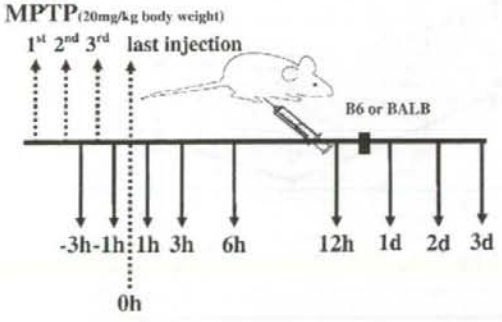

Fig. 1. Time schedule of acute MPTP treatment. MPTP was injected intraperitoneally into mice 4 times (1st, 2nd, 3rd, last) at 2-hour intervals. −3 h, −1 h, 1 h, 3 h, 6 h, and 12 h indicate −3, −1, 1, 3, 6, 12 h (where 0 h represents the time of last MPTP injection), and 1 d, 2 d and 3 d indicate days 1, 2 and 3 when mice were anesthetized for collection of CSF and plasma, and brain dissection.

2.2. Behavioral testing

MPTP effects on movement were evaluated by pole and bar tests according to the modified methods described by Kato et al. (Kato et al., 2004). Briefly, in the pole test, used for measuring motor coordination, the mice were placed head upwards near the top of a vertical wooden pole (diameter 10 mm, height 50 cm). The time required for the mice to turn completely downward (time to turn; T-turn), and to reach the floor (locomotion activity time; T-LA) were recorded with a cut-off limit of 30 s. To measure cataleptic symptoms, a bar-test was performed. These behavioral tests were examined on, before, and at 1, 3, 7, and 14 days after MPTP treatments. All values were expressed as mean ± SE and statistical significance was evaluated using the Student's *t*-test.

2.3. Immuno-histochemistry

Frozen sections (20 μm) were obtained on a cryostat (Yasuda et al., 2004). Marker proteins used in this study were: Thyrosin hydroxylase (TH) for DA neurons, Iba1 for microglia, and S100B for astrocytes. The following primary antibodies were prepared: rabbit anti-Iba1 polyclonal antibody (1/100, Wako, Osaka, Japan), rabbit anti-TH polyclonal antibody (1/200, Chemicon international, Inc., Temecula, CA, USA) and mouse anti-S100B monoclonal antibody (1/100, clone SH-B1, Sigama-Aldrich, USA). Secondary antibodies used were: Alexa Fluor® 488 goat anti-rabbit IgG $(Fab')_2$ and Alexa Fluor® 488 goat anti-mouse IgG $(Fab')_2$ (Molecular Probs, Eugene, OR, USA). After treatment with 0.3% triton X-100 in 0.1 M PB, sections were blocked in Blocking One (Nakarai Tesque, Kyoto, Japan) for 30 min. and incubated with the primary antibody overnight at 4 °C. After washing with 0.05% triton X-100 in PB, sections were incubated with the secondary antibodies for 1 h at room temperature (RT), washed with 0.05% triton X-100 in PB, mounted with Aqua Poly (Polysience AG, Cham, ZG, Switzerland) and observed under a confocal microscope (Flowview, Olympus, Tokyo, Japan). A single image was compiled by stacking four confocal images taken at 1 μm intervals. The TH^+ area in immunolabeled sections was analyzed with image analyses software (Cosmos32, Library Ltd. Tokyo, Japan) and the percentage of TH^+ area for gray matter in a part of the striatum was calculated as follows:

Percentage of TH^+ area (%) = (TH^+ area/gray matter) × 100%.

2.4. Measurement of S100B

A sandwich method was used to measure the concentration of S100B in CSF, according to the previously described method (Tateishi et al., 2002). Microtiter plates coated with an anti-S100B monoclonal antibody (1/1000, Clone SH-B4, Sigma-Aldrich, USA) were incubated overnight with standard bovine S100B protein (0.01–600 ng/ml; Calbiochem-Novabiochem, San Diego, CA, U.S.A) or samples at 4 °C. After triple-thorough washing with PBS, the plates were further incubated with an anti-S100 polyclonal antibody (1/1000, DAKO, Carpinteria, CA, USA) for 2 h at RT. ABC kit (Bio-Rad Laboratories, Inc., Hercules, CA, USA) was used for coloring. Biotinylated horse radish peroxidase was added to the plates, and the plates were then incubated for 2 h at RT. After triple-thorough washing with PBS, horseradish peroxidase substrate was finally added to the plates. After incubation for 5 min, the resulting absorbance was measured at an optical density of 412 nm.

2.5. Measurement of cytokine/chemokine in CSF and plasma

Cytokines/chemokines were detected using multiplexed fluorescent bead-based immunoassay. CSF was collected using glass capillaries (BSI-T1, Brain Science Idea, Osaka) and blood samples were taken from hearts. CSF and plasma samples were analyzed simultaneously for 23

Please cite this article as: Yasuda, Y., et al., The effects of MPTP on the activation of microglia/astrocytes and cytokine/chemokine levels in different mice strains, J. Neuroimmunol. (2008), doi:10.1016/j.jneuroim.2008.08.003

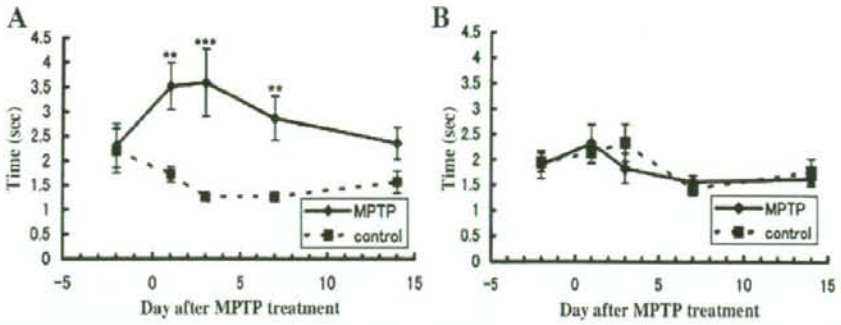

Fig. 2. MPTP effect on movement function A: pole test (T-turn) by B6. B: pole test (T-turn) by BALB. Values are expressed as mean ± SE. n = 8. * $0.1 > p > 0.05$, compared with control (vehicle treated) mice ** $0.05 > p > 0.005$, compared with control (vehicle treated) mice *** $p < 0.005$, compared with control (vehicle treated) mice.

different cytokines/chemokines, namely, using the Bio-Plex mouse 23-Plex Panel and the Bio-Plex Cytokine assay system (Bio-Rad Laboratories, Inc.) according to the manufacturer's instructions. Typically CSF and plasma samples were diluted 10-fold with serum dilution solution (Bio-Rad Laboratories Inc.). 50 μl of standards, CSF and serum samples were added to the wells which the beads (Bio-Plex mouse 23-Plex Panel) had been in. After 1 h of incubation and triple-thorough washing with wash buffer (Bio-Rad Laboratories, Inc.), 25 μl of biotinylated antibody reagent (Bio-Plex mouse 23-Plex Panel) was added to each well. After 30 min of incubation and triple-thorough washing with wash buffer, 50 μl of streptoavidin–phycoerythrin reagent (Bio-Plex mouse 23-Plex Panel) was added to the well. After 10 min of incubation and triple-thorough washing with wash buffer, 125 μl of cytokine assay buffer (Bio-Rad Laboratories, Inc.) was added to each well. Cytokine/chemokine concentrations were measured using Bio-Plex Array Reader (Bio-Rad Laboratories, Inc.) and calculated using a standard curve.

2.6. Statistical analysis

All values were expressed as mean ± SE. Paired student *t*-test was performed for comparison. Temporal alterations were analyzed by one-way ANOVA. The criterion for statistical significance was $p < 0.05$.

3. Results

3.1. Effect of MPTP on movement behavior

Alteration of behavior after MPTP treatment was compared between the highly MPTP-sensitive B6 and the less MPTP-sensitive BALB.

In B6, slowness of movement and salivation were observed after the second MPTP injection. Movement dysfunctions like rigidity and akinesia were also observed just after the last injection but disappeared within 24 h. In BALB, salivation appeared but no remarkable changes in movement were observed.

In order to evaluate movement dysfunction quantitatively, pole and bar tests were performed on days −2, 1, 3, 7 and 14 after the last MPTP injection. In MPTP-treated B6, a significant change in T-turn was observed (Fig. 2), albeit transiently. On the other hand, the MPTP-treated BALB exhibited no change in any test (Fig. 2).

3.2. Effect of MPTP on reduction of TH⁺ area in striatum

Fig. 3 shows the fluorescent images of TH expression in the striatum (Fig. 3, A) and the MPTP-induced reduction of the percentage of TH⁺ area in the gray matter of the striatum in B6 and BALB (Fig. 3, B).

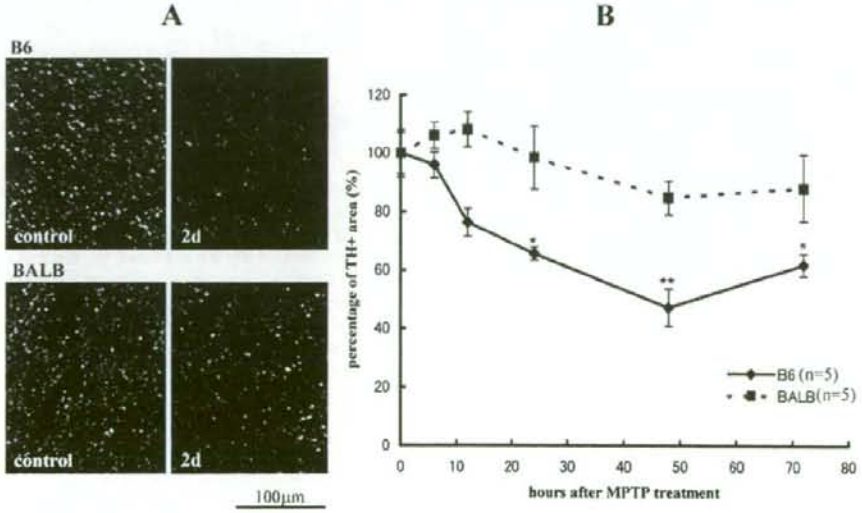

Fig. 3. Reduction of TH⁺ area in the striatum after MPTP treatment. A and B show the representative fluorescent images and the change of reduction rate of TH⁺ area in the striatum, respectively. Values are expressed as mean ± SE. n = 6. * $0.1 > p > 0.05$, compared with control (untreated) mice. ** $p < 0.05$, compared with control (untreated) mice.

Please cite this article as: Yasuda, Y., et al., The effects of MPTP on the activation of microglia/astrocytes and cytokine/chemokine levels in different mice strains, J. Neuroimmunol. (2008), doi:10.1016/j.jneuroim.2008.08.003

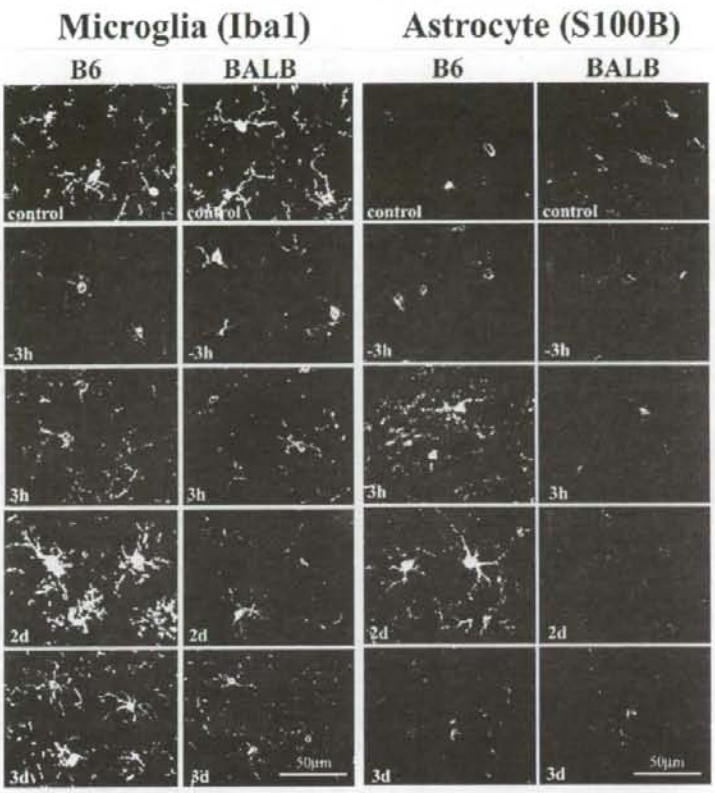

Fig. 4. Representative images of immunostaining with anti-Iba1 antibody and S100B in striatum after treatment with MPTP. Representative images were selected from images obtained by observing 5 mice at each time point. h and d indicate hours and days, respectively. Control indicates untreated, and −3 h, 3 h, 2 d, and 3 d indicate the time points after MPTP treatment. The processes of Iba1$^+$ microglia became thinner than that of the control in both B6 and BALB at −3 h. Iba1$^+$ big activated microglia with thick processes were observed only in B6 (2 d and 3 d), but not in BALB. S100B$^+$ activated astrocytes with thick processes were observed only in B6 (3 h and 2 d), but not in BALB. Transient increase of S100B immunostaining level was observed (3 h and 2 d) in B6, but not in BALB.

One-way ANOVA analysis indicated that after MPTP treatment, a significant reduction in the percentage of TH$^+$ area ($p<0.05$) in the gray matter of the striatum occurred at 12 h in B6, but not in BALB. This shows that neuronal injury had already started at 12 h in B6. These results also suggest the possibility that the events that induce DA neuronal death start before 12 h after MPTP injection.

3.3. Effect of MPTP on microglia

Alteration of microglia after MPTP treatment was studied in B6 and BALB, using an anti-Iba1 antibody. Morphological change was observed in both B6 and BALB after the second MPTP injection (Fig. 4: −3 h). The Iba1$^+$ processes of microglia were thinner in both MPTP-injected B6 and BALB than in untreated mice (Fig. 4, −3 h). Thereafter, in B6, the processes became increasingly thicker, and the cell bodies also became progressively enlarged until day 2 after the last injection (Fig. 4; 3 h, 2 d). Cell bodies and the processes of Iba1$^+$ activated microglia became thinner on day 3, in comparison to day 2 (Fig. 4; 2 d, 3 d). In BALB, the Iba1$^+$ processes became thicker up to 3 h after the last injection (Fig. 4, 3h). However, activated microglia with hypertrophic cell bodies and processes similar to that in B6 were not observed (Fig. 4; 2 d, 3 d).

These results indicate that although microglia respond abruptly to MPTP injection in both B6 and BALB, the additional MPTP injections promote microglia activation in B6 but not in BALB.

3.4. Effects of MPTP on S100B expression in astrocytes

Time dependent-alteration of S100B in astrocytes was examined immunohistochemically (Fig. 4). In B6, the S100B immunofluorescent level in astrocytes was higher at 1 h after the second MPTP injection (Fig. 4; -3h), as compared to the control. Afterward, the level increased gradually until day 2 after the last MPTP injection (Fig. 4, 2d). Strong S100B$^+$ activated astrocytes were observed, but on day 3, the S100B immunofluorescent level weakened in comparison to day 2 (Fig. 4; 3 h, 2 d, 3 d). In BALB, no remarkable changes were recognizable in S100B immunofluorescent level and morphology after MPTP treatment. These results indicate that a transient increase of S100B in astrocytes after MPTP treatment occurred in B6 but not in BALB.

We examined whether the increased S100B immunofluorescence in astrocytes was reflected by S100B concentration in the CSF on days 1, 2 and 3 after MPTP treatment (Fig. 5). On day 1, S100B level tended to be lower ($0.05<p<0.1$) and on day 2, it was still significantly lower, compared to the control in B6 ($p<0.05$), while no change was observed in BALB.

3.5. Cytokine/chemokine concentrations in CSF and plasma after MPTP treatment

Using a multiplex system, 23 cytokines/chemokines in the CSF were examined. The cytokines examined were: IL-1α, IL-1β, IL-2, IL-3,

Please cite this article as: Yasuda, Y., et al., The effects of MPTP on the activation of microglia/astrocytes and cytokine/chemokine levels in different mice strains, J. Neuroimmunol. (2008), doi:10.1016/j.jneuroim.2008.08.003

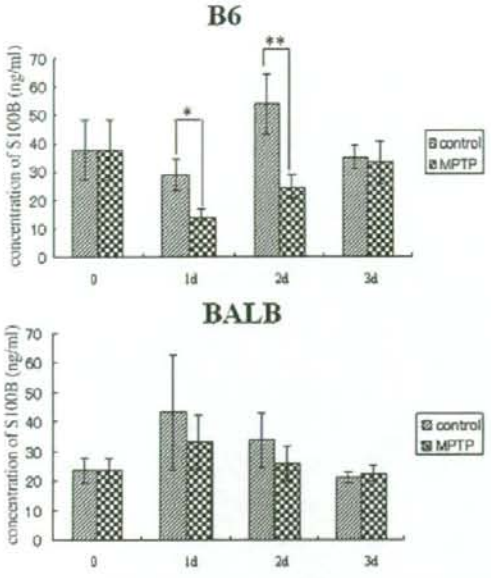

Fig. 5. Change in S100B concentration in CSF after MPTP treatment. Values are expressed as mean±SE. $n=4$. *$0.1>p>0.05$, compared with control (untreated) mice. ** $p<0.05$, compared with control (untreated) mice.

IL-4, IL-5, IL-6, IL-9, IL-10, IL-12(p40), IL-12(p70), IL-13, IL-17, granulocyte-colony stimulating factor (G-CSF), granulocyte-macrophage colony-stimulating factor (GM-CSF), IFN-γ and TNF-α. The chemokines examined were: chemoattractant of eosinophil (EOTAXIN), chemoattractant of neutrophil (KC), MCP-1, MIP-1α, MIP-1β, and regulated upon activation, normal T cell expressed and secreted protein (RANTES).

Table 1
Strain differences in cytokine/chemokine concentrations in CSF and plasma of untreated mice

	B6>BALB		B6=BALB	B6<BALB	
	$p<0.05$	$0.05<P<0.1$	$0.1\leq p\leq 0.9$	$0.1>p>0.05$	$0.05>p$
CSF			IL-1β, IL-5, IL-10, EOTAXIN, GM-CSF, MIP-1α, IFN-γ, MCP-1, MIP-1β,	IL-9, IL-12 (p40), TNF-α	IL-1α, IL-2, IL-4, IL-6, IL-12(p70), IL-13, IL-17, KC,
PLASMA	IL-2, IL-10, G-CSF, GM-CSF, MIP-1α	IL-12(p40), IL-13, RANTES, TNF-α	IL-1α, IL-1β, IL-5, IL-9, EOTAXIN, IFN-γ, MCP-1		KC

This table shows the comparison of cytokine/chemokine concentrations in CSF or plasma between B6 and BALB, based on Fig. 6. *t*-tests between the concentrations of B6 and BALB. $0<0.05$: significantly different, $0.1>p>0.05$: different but not statistically significant, ns: not significantly different.

The cytokine/chemokine concentrations in CSF and plasma were first compared with that of normal B6 and BALB (Fig. 6, Table 1). There were some differences between cytokine/chemokine concentrations in the CSF and plasma of B6 and BALB. (Table 1). In comparison to B6, the CSF of BALB showed significantly higher ($p<0.05$) concentrations of IL-1α, IL-2, IL-4, IL-6, IL-12 (p70), IL-13, IL-17 and KC, while concentrations of IL-9, IL-12(p40), and TNF-α were higher but not statistically significant ($0.05<p<0.1$)(Fig. 6, Table 1). In comparison to BALB, the plasma of B6 showed significantly ($p<0.05$) higher concentrations of IL-2, IL-10, G-CSF, GM-CSF and MIP-1α while concentrations of IL-12(p40), IL-13, RANTES and TNF-α were high but not statistically significant ($0.05<p<0.1$)(Fig. 6, Table 1). Thus,

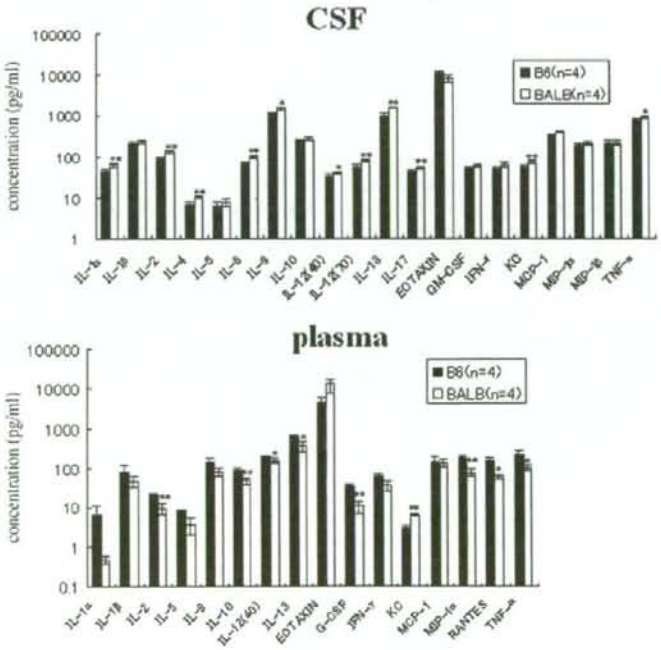

Fig. 6. Cytokine/chemokine concentrations in CSF and plasma of untreated B6 and BALB. Values of the measured cytokines/chemokines that were not described in this graph were below the measurement limitation. Values are expressed as mean±SE. $n=4$. *: $0.1>p>0.05$, compared between B6 and BALB. **: $p<0.05$, compared between B6 and BALB.

Please cite this article as: Yasuda, Y., et al., The effects of MPTP on the activation of microglia/astrocytes and cytokine/chemokine levels in different mice strains, J. Neuroimmunol. (2008), doi:10.1016/j.jneuroim.2008.08.003

differences between normal B6 and BALB were observed in the cytokine/chemokine concentrations in both CSF and plasma.

Based on reports that the mRNA expression of proinflammatory cytokines (IL-1α, IL-1β, IL-6, and TNF-α) in the striatum peaks on day 1 after MPTP treatment (Hebert et al., 2003), a comparison of cytokine/chemokine concentrations in CSF and plasma was performed between MPTP-treated mice and the corresponding controls on days 1 and 3 after MPTP treatment. After day 1, alterations in some cytokine/chemokine concentrations in both CSF and plasma were found to be different between B6 and BALB (Figs. 7 and 8, Table 2). In the CSF of MPTP-treated B6, IL-10, IL-12(p40), IL-13, IFN-γ and MCP-1 were found at significantly high concentrations, while that of TNF-α although still higher was not statistically significant as compared to the control (Fig. 7, Table 2). In the CSF of MPTP-treated BALB, however, none of the cytokines/chemokines exhibited higher concentration than the control. The concentration of IL-17 was significantly lower ($p<0.05$) than the control, and IL-12(p40) was also lower but not statistically significant, as compared to the control (Fig. 7, Table 2). In the plasma of B6 or BALB, none of the cytokines/chemokines were elevated when compared with the control (Fig. 8, Table 2). The concentrations of IL-12(p40) in B6, and IL-1β, IL-10 and IL-12(p40) in BALB were lower than the control (Fig. 8, Table 2). After 3 days, measurable cytokine/chemokine concentrations in CSF and plasma showed no differences between MPTP-treated mice and the control (data not shown). These results may be compatible to the morphological changes in microglia/astrocytes that occurred between day 2 and day 3 after MPTP treatment.

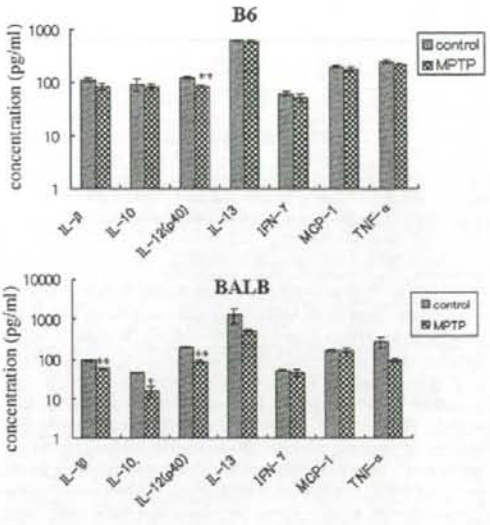

Fig. 8. Cytokine/chemokine concentrations of plasma at 24 h after MPTP treatment Values of the measured cytokines/chemokines that were not described in this graph were not significantly different between MPTP-treated and control mice or were below the measurement limitation. Values are expressed as mean±SE. $n=5$ *: $0.1>p>0.05$, compared with control (vehicle treated) mice **: $p<0.05$, compared with control (vehicle treated) mice.

4. Discussion

We found that: 1) movement dysfunction and activated microglia/astrocytes were induced by MPTP in highly MPTP-sensitive B6 with a propensity for Th1 but not in less MPTP-sensitive BALB with a propensity for Th2 and; 2) the changes in cytokine/chemokine concentrations in CSF after MPTP treatment were different between B6 and BALB. These observations suggest that activation of microglia/astrocytes and immunological response contribute to PD development and that the variations in immunological background might be related to sensitivity differences to MPTP.

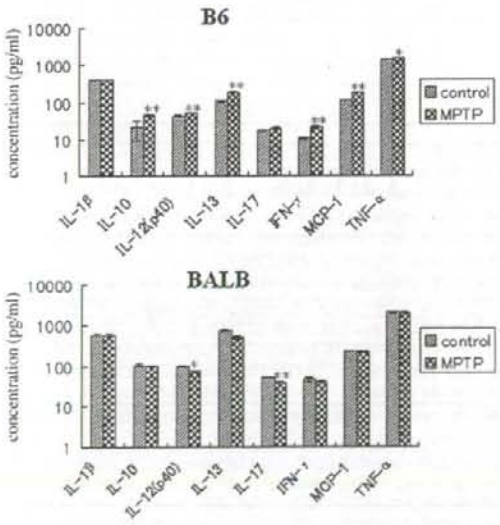

Fig. 7. Cytokine/chemokine concentrations of CSF at 24 h after MPTP treatment. Values of the measured cytokines/chemokines that were not described in this graph were not significantly different between MPTP-treated and control mice or were below the measurement limitation. Values are expressed as mean±SE. $n=5$. *: $0.1>p>0.05$, compared with control (vehicle treated) mice. **: $p<0.05$, compared with control (vehicle treated) mice.

4.1. Movement dysfunction and reduction of TH⁺ area

MPTP-induced movement dysfunction and reduction of the percentage of TH⁺ area were observed in B6 with high MPTP-sensitivity, but not in BALB with less MPTP-sensitivity (Yasuda et al., 2007). MPTP-induced movement behavior changes occurred prior to the reduction in the TH⁺ area. These results indicate that the severity of movement dysfunction observed shortly after MPTP treatment is reflected by the reduction of the TH⁺ area.

4.2. Activation of microglia/astrocytes

A slight morphological change in microglia/astrocytes was recognized 1 h after the second MPTP injection (−3 h) in both B6 and BALB, indicating that microglia/astrocytes respond immediately to MPTP injection in both B6 and BALB. However, additional MPTP injections promote the activation of microglia/astrocytes only in B6, and not in BALB. These results suggest that activation of microglia (Du et al., 2001; Wu et al., 2002)/astrocytes may be associated with DA neuron loss.

Activation of astrocytes in B6 was accompanied by a transient increase of S100B expression: S100B released from astrocytes generally has a role in maintaining homeostasis of the brain environment. Extracellular S100B creates a double-edged sword effect; it has a beneficial effect at low MPTP concentrations (nM level), but a deleterious effect at high MPTP concentrations (μM level). (Van Eldik and Wainwright, 2003). We have previously reported that an increase in S100B concentration in CSF and an increase of S100B expression in astocytes were related to cell death resulting in infarct expansion (Matsui et al., 2002; Yasuda et al., 2004). S100B concentration in serum or CSF also increases in other traumatic brain conditions (Sheng et al., 1996; Wunderlich et al., 1999; Yasuda

Please cite this article as: Yasuda, Y., et al., The effects of MPTP on the activation of microglia/astrocytes and cytokine/chemokine levels in different mice strains, J. Neuroimmunol. (2008), doi:10.1016/j.jneuroim.2008.08.003

Table 2
Change of cytokine/chemokine concentrations in CSF and plasma at 24 h after MPTP treatment

		IL-1β	IL-10	IL-12(p40)	IL-13	IL-17	IFN-γ	MCP-1	TNF-α
CSF	B6	ns	$p<0.05$↑	$p<0.05$↑	$p<0.05$↑	ns	$p<0.05$↑	$p<0.05$↑	$0.1>p>0.05$↑
	BALB	ns	ns	$0.1>p>0.05$↓	ns	$p<0.05$↓	ns	ns	ns
Plasma	B6	ns	ns	$p<0.05$↓	ns	ns	ns	ns	ns
	BALB	$p<0.05$↓	$0.1>p>0.05$↓	$p<0.05$↓	ns	ns	ns	ns	ns

This table shows the comparison of cytokine/chemokine concentrations in CSF or plasma between MPTP treated and control (vehicle treated) mice, based on Figs. 7 and 8. *t*-test between the concentrations in CSF or plasma of control and MPTP treated mice at 24 h after MPTP treatment. $0<0.05$: significantly different, $0.1>p>0.05$: different but not statistically significant, ns: not significantly different, ↑: increase, ↓: decrease.

et al., 2004). In this study, rather than being higher, the S100B concentration in the CSF of MPTP-treated B6 was found to be lower than the control. S100B concentration in the CSF of BALB did not change after MPTP treatment. In *in vitro* experiments using coculture of C6 rat glioma cells (C6) and PC12 rat pheochromocytoma cells (PC12), MPTP increased S100B production in C6 and reduced the viability of PC12. An antibody against S100B suppressed these phenomena, suggesting that S100B induced by MPTP contributes to neurotoxicity (Iuvone et al., 2007). Although the S100B concentration in the CSF of B6 was lower than that of the control in the present experiment, S100B concentration in SNpc might have been higher, resulting in the loss of DA neurons. A previous report has shown that patients with clinically less severe PD exhibit lower level of S100B (Schaf et al., 2005), suggesting that PD patients, at the onset of the disease, have lower level of S100B (Schaf et al., 2005). The reduction of S100B concentration in the CSF on days 1 and 2 after MPTP treatment is thought to reflect a phenomenon occurring in the early stages of PD pathogenesis. But how this reduction is connected to PD pathogens remains to be explained. Strong S100B positive astrocytes in MPTP-treated B6 indicate that S100B may be produced in order to compensate for the shortage and to maintain homeostasis of S100B in the nigra-striatal pathway, or that astrocytes may be in the G1 phase of the cell cycle and an increase of S100B production may be related to the proliferation of astrocytes (Baudier et al., 1992).

It has been reported that astrocytes regulate immunological responses and influence IL-6 and TNF-α secretion in the CNS (Farina et al., 2007; Muramatsu et al., 2003; Schmitt et al., 2007). In PD pathogenesis, S100B might contribute to the regulation of cytokine production. Transgenic mice that completely lack S100B develop normally and there was no detectable abnormality in the histological architecture of the mutant brain (Nishiyama et al., 2002). How a reduction in S100B concentration is connected to PD pathogenesis remains unclear. To clarify how the transient increase of S100B expression in astrocytes, the reduction of S100B level in CSF, and the regulation of cytokine production by S100B are associated with trophic or toxic effects to the DA neuronal cells, and how S100B regulates cytokine production in PD pathogenesis will require more study (Gomide and Chadi, 1999; Himeda et al., 2006).

4.3. Cytokine/chemokine

The difference between highly MPTP-sensitive B6 with a propensity for Th1, and less MPTP-sensitive BALB with a propensity for Th2, was reflected in some cytokine/chemokine concentrations in normal CSF or plasma, and in the alteration of some cytokine/chemokine concentrations in CSF after MPTP-treatment.

Increases of inflammatory cytokines/chemokines in PD patients and animal models have been reported (Hunot and Hirsch, 2003; Liu, 2006; Nagatsu and Sawada, 2005). In the PD mouse model, concentrations of IL-1α, IL-1β, IL-6, TNF-α, MCP-1, MIP-1α and MIP-1β or their mRNA expression increase in the nigra-striatal pathway (Hebert et al., 2003; Kalkonde et al., 2007; Liu, 2006; Pattarini et al., 2007). However, there are no reports on the cytokine/chemokine levels in the CSF of the PD mouse model.

To our knowledge, this is the first report describing cytokine/chemokine concentrations in the CSF of normal and MPTP-treated mice. Increases of IL-10, IL-12(p40), IL-13, IFN-γ, MCP-1 and TNF-α on day 1 after MPTP treatment were observed in the CSF of highly MPTP-sensitive B6 but not in that of BALB. In BALB, no increase in any of the cytokine/chemokine concentrations in CSF was detected, with IL-12 (p40) and IL-17 levels that were lower than that in the control. These results suggest that increased concentrations of cytokine/chemokine that occurred after MPTP treatment might be related to PD pathogenesis, while the decrease of cytokine/chemokine concentrations that occurred after MPTP might be related to suppression of PD development. The fact that no cytokine/chemokine concentrations were elevated in the plasma, suggests that alteration of cytokine/chemokine levels in the plasma may not necessarily be associated with PD development.

In contrast to previous reports on the nigra-striatum, we did not detect any increase in levels of IL-1α, IL-1β, IL-6, MIP-1α and MIP-1β in CSF in our experiments. The difference between cytokine/chemokine changes in the CSF and the nigra-striatal pathway could not be explained, but the increases in IL-10, IL-12(p40), IL-13, IFN-γ MCP-1 and TNF-α in the CSF are likely to be related to the progression of DA neuronal death. IL-12(p40), IFN-γ, MCP-1 and TNF-α are pro-inflammatory cytokines/chemokines. IL-12(p40), IFN-γ and TNF-α are Th1 cytokines. IFN-γ participates in the death of DA neurons by regulating microglia activity (Mount et al., 2007). TNF-α synthesized in microglia plays a role in DA neuronal death. Monomeric IL-12 (p40), produced in microglia, is secreted in excess by activated microglia, compared with the secretion of the heterodimeric IL-12(p70) (dimer of IL-12(p35) and (p40)). The significance of IL-12(p40) secretion is still unclear but IL-12(p70) is a central regulator of immune response and is thought to be implicated in the pathogenesis of certain inflammatory CNS diseases (Aloisi et al., 1997). If an increase in IL-12(p40) production is comparable to an increased production of IL-12(p70) (Hessle et al., 1999), the increase of IL-12(p40) concentration in CSF might suggest an increased level of IL-12(p70) in the nigra-striatal pathway which might be associated with PD pathogenesis. Production of MCP-1, implicated in several neurodegenerative and retrograde degenerative conditions (Perrin et al., 2005), is the earliest response to MPTP and localized in the DA neurons (Banisadr et al., 2005) and astrocytes (Kalkonde et al., 2007). In MCP-1 and a receptor of MCP-1 (CCR2) double knockout mice, the reduction of TH^+ neurons was comparable with that of wild type mice (Pattarini et al., 2007). Pattarini et al., 2007 suggested that MCP-1 might not be connected with the loss of DA neurons by MPTP. However, several cytokines/chemokine are produced during the inflammatory processes in PD. Inhibiting only one cytokine or chemokine in the pathway may not be sufficient for the protection of DA neurons against degeneration. IL-10 and IL-13 are among the Th2 cytokines. IL-10 is one of the anti-inflammatory cytokines that inhibit activation of microglia and their production of TNF-α (Aloisi et al., 1999). Th1 cells are believed to induce brain inflammation and Th2 cells are thought to be anti-inflammatory (Kuchroo et al., 2002). Th1 cytokine (TNF-α and IL-2) and Th2 cytokine (IL-4 and IL-6) levels in the CSF are also known to increase in PD patients, compared to control subjects (Hunot and Hirsch, 2003), implicating the Th1/Th2 cytokine

Please cite this article as: Yasuda, Y., et al., The effects of MPTP on the activation of microglia/astrocytes and cytokine/chemokine levels in different mice strains, J. Neuroimmunol. (2008), doi:10.1016/j.jneuroim.2008.08.003

balance in PD pathogenesis. How cytokines/chemokines orchestrate processes that lead to the loss of DA neurons remain unclear. The balance of Th1 and Th2 might lead to inflammation related with PD pathogenesis in B6 by MPTP. Even if the increase of Th2 cytokines observed at 24 h after MPTP treatment, the balance between Th1 and Th2 might become Th1 dominant and lead to inflammation, resulting in the loss of DA neurons in SNpc of B6.

MPTP is mitochondrial toxicant and induces a reduction of ATP and an increase of reactive oxygen species, leading to the death of DA neurons (Bezard et al., 1999; Przedborski and Ischiropoulos, 2005). Inhibition of microglial activation or inflammation attenuates the loss of DA neurons (Wahner et al., 2007). Together, oxidative-stress-induced signaling and neuroinflammatory responses may contribute to the loss of DA neurons in the SNpc in PD patients and MPTP induced animal model (Hunot and Hirsch, 2003; Jackson-Lewis and Smeyne, 2005). In this comparative study between B6 and BALB, we suggested that immunological background might contribute to strain difference in MPTP-sensitivity. There are reports that discuss strain difference of MPTP sensitivity in aspects of oxidative stress (Boyd et al., 2007; Smeyne et al., 2007). In comparative studies between B6 and MPTP resistant SW, no base line difference was found in levels of MPP^+, DAT and VMAT2 protein between them, suggesting the ability that DA neurons might be resistant to oxidative stress (Boyd et al., 2007). Any experiments to compare the processing of oxidative stress between B6 and BALB have not been performed yet. It would be necessary to make clear how oxidative signaling is related to inflammation, leading to PD pathogenesis.

Acknowledgments

We thank Dr. Ruth Yu for her advice in preparation of this manuscript.

References

Aloisi, F., Penna, G., Cerase, J., Menendez Iglesias, B., Adorini, L., 1997. IL-12 production by central nervous system microglia is inhibited by astrocytes. J. Immunol. 159, 1604–1612.

Aloisi, F., De Simone, R., Columba-Cabezas, S., Levi, G., 1999. Opposite effects of interferon-gamma and prostaglandin E2 on tumor necrosis factor and interleukin-10 production in microglia: a regulatory loop controlling microglia pro- and anti-inflammatory activities. J. Neurosci. Res. 56, 571–580.

Banisadr, G., Gosselin, R.D., Mechighel, P., Kitabgi, P., Rostene, W., Parsadaniantz, S.M., 2005. Highly regionalized neuronal expression of monocyte chemoattractant protein-1 (MCP-1/CCL2) in rat brain: evidence for its colocalization with neurotransmitters and neuropeptides. J. Comp. Neurol. 489, 275–292.

Barcia, C., Fernandez Barreiro, A., Poza, M., Herrero, M.T., 2003. Parkinson's disease and inflammatory changes. Neurotox. Res. 5, 411–418.

Baudier, J., Delphin, C., Grunwald, D., Khochbin, S., Lawrence, J.J., 1992. Characterization of the tumor suppressor protein p53 as a protein kinase C substrate and a S100b-binding protein. Proc. Natl. Acad. Sci. U. S. A. 89, 11627–11631.

Bezard, E., Gross, C.E., Fournier, M.C., Dovero, S., Bloch, B., Jaber, M., 1999. Absence of MPTP-induced neuronal death in mice lacking the dopamine transporter. Exp. Neurol. 155, 268–273.

Boyd, J.D., Jang, H., Shepherd, K.R., Faherty, C., Slack, S., Jiao, Y., Smeyne, R.J., 2007. Response to 1-methyl-4-phenyl-1,2,3,6-tetrahydropyridine (MPTP) differs in mouse strains and reveals a divergence in JNK signaling and COX-2 induction prior to loss of neurons in the substantia nigra pars compacta. Brain Res. 1175, 107–116.

Carpentier, P.A., Begolka, W.S., Olson, J.K., Elhofy, A., Karpus, W.J., Miller, S.D., 2005. Differential activation of astrocytes by innate and adaptive immune stimuli. Glia 49, 360–374.

Carvey, P.M., Chen, E.Y., Lipton, J.W., Tong, C.W., Chang, Q.A., Ling, Z.D., 2005. Intraparenchymal injection of tumor necrosis factor-alpha and interleukin 1-beta produces dopamine neuron loss in the rat. J. Neural Transm. 112, 601–612.

Chen, H., Zhang, S.M., Heman, M.A., Schwarzschild, M.A., Willett, W.C., Colditz, G.A., Speizer, F.E., Ascherio, A., 2003. Nonsteroidal anti-inflammatory drugs and the risk of Parkinson disease. Arch. Neurol. 60, 1059–1064.

Chiba, K., Trevor, A.J., Castagnoli Jr., N., 1985. Active uptake of MPP+, a metabolite of MPTP, by brain synaptosomes. Biochem. Biophys. Res. Commun. 128, 1228–1232.

Du, Y., Ma, Z., Lin, S., Dodel, R.C., Gao, F., Bales, K.R., Triarhou, L.C., Chernet, E., Perry, K.W., Nelson, D.L., Luecke, S., Phebus, L.A., Bymaster, F.P., Paul, S.M., 2001. Minocycline prevents nigrostriatal dopaminergic neurodegeneration in the MPTP model of Parkinson's disease. Proc. Natl. Acad. Sci. U. S. A. 98, 14669–14674.

Farina, C., Aloisi, F., Meinl, E., 2007. Astrocytes are active players in cerebral innate immunity. Trends Immunol. 28, 138–145.

Gomide, V.C., Chadi, G., 1999. The trophic factors S-100beta and basic fibroblast growth factor are increased in the forebrain reactive astrocytes of adult callosotomized rat. Brain Res. 835, 162–174.

Hebert, G., Arsaut, J., Dantzer, R., Demotes-Mainard, J., 2003. Time-course of the expression of inflammatory cytokines and matrix metalloproteinases in the striatum and mesencephalon of mice injected with 1-methyl-4-phenyl-1,2,3,6-tetrahydropyridine, a dopaminergic neurotoxin. Neurosci. Lett. 349, 191–195.

Heinzel, F.P., Sadick, M.D., Holaday, B.J., Coffman, R.L., Locksley, R.M., 1989. Reciprocal expression of interferon gamma or interleukin 4 during the resolution or progression of murine leishmaniasis. Evidence for expansion of distinct helper T cell subsets. J. Exp. Med. 169, 59–72.

Hessle, C., Hanson, L.A., Wold, A.E., 1999. Lactobacilli from human gastrointestinal mucosa are strong stimulators of IL-12 production. Clin. Exp. Immunol. 116, 276–282.

Himeda, T., Watanabe, Y., Tounai, H., Hayakawa, N., Kato, H., Araki, T., 2006. Time dependent alterations of co-localization of S100beta and GFAP in the MPTP-treated mice. J. Neural Transm. 113, 1887–1894.

Hirsch, E.C., Hunot, S., Damier, P., Brugg, B., Faucheux, B.A., Michel, P.P., Ruberg, M., Muriel, M.P., Mouatt-Prigent, A., Agid, Y., 1999. Glial cell participation in the degeneration of dopaminergic neurons in Parkinson's disease. Adv. Neurol. 80, 9–18.

Hunot, S., Hirsch, E.C., 2003. Neuroinflammatory processes in Parkinson's disease. Ann. Neurol. 53 (Suppl 3), S49–S58 discussion S58–60.

Iuvone, T., Esposito, G., De Filippis, D., Bisogno, T., Petrosino, S., Scuderi, C., Di Marzo, V., Steardo, L., 2007. Cannabinoid CB1 receptor stimulation affords neuroprotection in MPTP-induced neurotoxicity by attenuating S100B up-regulation in vitro. J. Mol. Med. 85, 1379–1392.

Jackson-Lewis, V., Jakowec, M., Burke, R.E., Przedborski, S., 1995. Time course and morphology of dopaminergic neuronal death caused by the neurotoxin 1-methyl-4-phenyl-1,2,3,6-tetrahydropyridine. Neurodegeneration 4, 257–269.

Jackson-Lewis, V., Smeyne, R.J., 2005. MPTP and SNpc DA neuronal vulnerability: role of dopamine, superoxide and nitric oxide in neurotoxicity. Minireview. Neurotox. Res. 7, 193–202.

Kalkonde, Y.V., Morgan, W.W., Sigala, J., Maffi, S.K., Condello, C., Kuziel, W., Ahuja, S.S., Ahuja, S.K., 2007. Chemokines in the MPTP model of Parkinson's disease: absence of CCL2 and its receptor CCR2 does not protect against striatal neurodegeneration. Brain Res. 1128, 1–11.

Kato, H., Kurosaki, R., Oki, C., Araki, T., 2004. Arundic acid, an astrocyte-modulating agent, protects dopaminergic neurons against MPTP neurotoxicity in mice. Brain Res. 1030, 66–73.

Kim, Y.S., Joh, T.H., 2006. Microglia, major player in the brain inflammation: their roles in the pathogenesis of Parkinson's disease. Exp. Mol. Med. 38, 333–347.

Kuchroo, V.K., Anderson, A.C., Waldner, H., Munder, M., Bettelli, E., Nicholson, L.B., 2002. T cell response in experimental autoimmune encephalomyelitis (EAE): role of self and cross-reactive antigens in shaping, tuning, and regulating the autopathogenic T cell repertoire. Annu. Rev. Immunol. 20, 101–123.

Liu, B., 2006. Modulation of microglial pro-inflammatory and neurotoxic activity for the treatment of Parkinson's disease. Aaps J. 8, E606–621.

Matsui, T., Mori, T., Tateishi, N., Kagamiishi, Y., Satoh, S., Katsube, N., Morikawa, E., Morimoto, T., Ikuta, F., Asano, T., 2002. Astrocytic activation and delayed infarct expansion after permanent focal ischemia in rats. Part I: enhanced astrocytic synthesis of s-100beta in the periinfarct area precedes delayed infarct expansion. J. Cereb. Blood Flow Metab. 22, 711–722.

Mosmann, T.R., Sad, S., 1996. The expanding universe of T-cell subsets: Th1, Th2 and more. Immunol. Today 17, 138–146.

Mount, M.P., Lira, A., Grimes, D., Smith, P.D., Faucher, S., Slack, R., Anisman, H., Hayley, S., Park, D.S., 2007. Involvement of interferon-gamma in microglial-mediated loss of dopaminergic neurons. J. Neurosci. 27, 3328–3337.

Muramatsu, Y., Kurosaki, R., Watanabe, H., Michimata, M., Matsubara, M., Imai, Y., Araki, T., 2003. Expression of S-100 protein is related to neuronal damage in MPTP-treated mice. Glia 42, 307–313.

Nagatsu, T., Sawada, M., 2005. Inflammatory process in Parkinson's disease: role for cytokines. Curr. Pharm. Des. 11, 999–1016.

Nishiyama, H., Takemura, M., Takeda, T., Itohara, S., 2002. Normal development of serotonergic neurons in mice lacking S100B. Neurosci. Lett. 321, 49–52.

Pattarini, R., Smeyne, R.J., Morgan, J.I., 2007. Temporal mRNA profiles of inflammatory mediators in the murine 1-methyl-4-phenyl-1,2,3,6-tetrahydropyrimidine model of Parkinson's disease. Neuroscience 145, 654–668.

Perrin, F.E., Lacroix, S., Aviles-Trigueros, M., David, S., 2005. Involvement of mo yte chemoattractant protein-1, macrophage inflammatory protein-1alpha and ter-leukin-1beta in Wallerian degeneration. Brain 128, 854–866.

Przedborski, S., Ischiropoulos, H., 2005. Reactive oxygen and nitrogen species: weal ns of neuronal destruction in models of Parkinson's disease. Antioxid. Redox Sign. , 7, 685–693.

Przedborski, S., Jackson-Lewis, V., Naini, A.B., Jakowec, M., Petzinger, G., Mille R., Akram, M., 2001. The parkinsonian toxin 1-methyl-4-phenyl-1,2,3,6-tetrahyuro-pyridine (MPTP): a technical review of its utility and safety. J. Neurochem. 76, 1265–1274.

Sawada, M., Imamura, K., Nagatsu, T., 2006. Role of cytokines in inflammatory process in Parkinson's disease. J. Neural Transm., Suppl. 373–381.

Schaf, D.V., Tort, A.B., Fricke, D., Schestatsky, P., Portela, L.V., Souza, D.O., Rieder, C.R., 2005. S100B and NSE serum levels in patients with Parkinson's disease. Parkinsonism Relat. Disord. 11, 39–43.

Schmitt, K.R., Kern, C., Lange, P.E., Berger, F., Abdul-Khaliq, H., Hendrix, S., 2007. S100B modulates IL-6 release and cytotoxicity from hypothermic brain cells and inhibits hypothermia-induced axonal outgrowth. Neurosci. Res. 59, 68–73.

Please cite this article as: Yasuda, Y., et al., The effects of MPTP on the activation of microglia/astrocytes and cytokine/chemokine levels in different mice strains, J. Neuroimmunol. (2008), doi:10.1016/j.jneuroim.2008.08.003

Sedelis, M., Hofele, K., Auburger, G.W., Morgan, S., Huston, J.P., Schwarting, R.K., 2000. MPTP susceptibility in the mouse: behavioral, neurochemical, and histological analysis of gender and strain differences. Behav. Genet. 30, 171–182.

Sheng, J.G., Mrak, R.E., Rovnaghi, C.R., Kozlowska, E., Van Eldik, L.J., Griffin, W.S., 1996. Human brain S100 beta and S100 beta mRNA expression increases with age: pathogenic implications for Alzheimer's disease. Neurobiol. Aging 17, 359–363.

Smeyne, M., Boyd, J., Raviie Shepherd, K., Jiao, Y., Pond, B.B., Hatler, M., Wolf, R., Henderson, C., Smeyne, R.J., 2007. GSTpi expression mediates dopaminergic neuron sensitivity in experimental parkinsonism. Proc. Natl. Acad. Sci. U. S. A. 104, 1977–1982.

Tateishi, N., Mori, T., Kagamiishi, Y., Satoh, S., Katsube, N., Morikawa, E., Morimoto, T., Matsui, T., Asano, T., 2002. Astrocytic activation and delayed infarct expansion after permanent focal ischemia in rats. Part II: suppression of astrocytic activation by a novel agent (R)-(−)-2-propyloctanoic acid (ONO-2506) leads to mitigation of delayed infarct expansion and early improvement of neurologic deficits. J. Cereb. Blood Flow Metab. 22, 723–734.

Teismann, P., Schulz, J.B., 2004. Cellular pathology of Parkinson's disease: astrocytes, microglia and inflammation. Cell Tissue Res. 318, 149–161.

Van Eldik, L.J., Wainwright, M.S., 2003. The Janus face of glial-derived S100B: beneficial and detrimental functions in the brain. Restor. Neurol. Neurosci. 21, 97–108.

Wahner, A.D., Bronstein, J.M., Bordelon, Y.M., Ritz, B., 2007. Nonsteroidal anti-inflammatory drugs may protect against Parkinson disease. Neurology 69, 1836–1842.

Wu, D.C., Jackson-Lewis, V., Vila, M., Tieu, K., Teismann, P., Vadseth, C., Choi, D.K., Ischiropoulos, H., Przedborski, S., 2002. Blockade of microglial activation is neuroprotective in the 1-methyl-4-phenyl-1,2,3,6-tetrahydropyridine mouse model of Parkinson disease. J. Neurosci. 22, 1763–1771.

Wunderlich, M.T., Ebert, A.D., Kratz, T., Goertler, M., Jost, S., Herrmann, M., 1999. Early neurobehavioral outcome after stroke is related to release of neurobiochemical markers of brain damage. Stroke 30, 1190–1195.

Yasuda, Y., Tateishi, N., Shimoda, T., Satoh, S., Ogitani, E., Fujita, S., 2004. Relationship between S100beta and GFAP expression in astrocytes during infarction and glial scar formation after mild transient ischemia. Brain Res. 1021, 20–31.

Yasuda, Y., Shinagawa, R., Yamada, M., Mori, T., Tateishi, N., Fujita, S., 2007. Long-lasting reactive changes observed in microglia in the striatal and substantia nigral of mice after 1-methyl-4-phenyl-1,2,3,6-tetrahydropyridine. Brain Res. 1138, 196–202.

Please cite this article as: Yasuda, Y., et al., The effects of MPTP on the activation of microglia/astrocytes and cytokine/chemokine levels in different mice strains, J. Neuroimmunol. (2008), doi:10.1016/j.jneuroim.2008.08.003

Requirement for Vav Proteins in Post-Recruitment Neutrophil Cytotoxicity in IgG but Not Complement C3-Dependent Injury[1]

Ahmad Utomo,[2]* Junichi Hirahashi,[2]* Divya Mekala,[2]* Kenichi Asano,* Michael Glogauer,† Xavier Cullere,* and Tanya N. Mayadas[3]*

The signals linking neutrophil opsonic receptors, FcγRs and complement receptor 3 (Mac-1) to cellular cytotoxic responses are poorly understood. Furthermore, because a deficiency in activating FcγRs reduces both IgG-mediated neutrophil recruitment and tissue injury, the role of FcγRs specifically in mediating neutrophil cytotoxicity in vivo remains unclear. In this study, we demonstrate that neutrophil Vav 1 and 3, guanine exchange factors for Rac GTPases, are required for IgG/FcγR-mediated hemorrhage and edema in the reverse passive Arthus in the lung and skin. Rac GTPases are also required for development of the reverse passive Arthus reaction. A deficiency in Vav 1 and 3 does not affect neutrophil accumulation at the site of immune complex deposition, thus uncoupling neutrophil recruitment and tissue injury. Surprisingly, Vav and Rac proteins are dispensable for the development of the local Shwartzman reaction in vivo and phagocytosis of complement-opsonized RBC in vitro, processes strictly dependent on Mac-1 and complement C3. Thus, FcγR signaling through the Vav and Rac proteins in neutrophils is critical for stimulating immune complex disease while Vav- and Rac-independent pathways promote Mac-1/complement C3-dependent functions. *The Journal of Immunology,* **2008, 180: 6279–6287.**

Neutrophils express two major opsonic receptors, FcγR and complement receptor 3, also known as the β_2 integrin Mac-1 (CD11b/CD18), that engage IgG and complement fragment iC3b-opsonized targets, respectively (1). Recent data suggest that tissue injury associated with IgG and/or complement deposition in tissue may be attributed to the activity of these receptors. A deficiency in activating FcγRs protects from immune complex (IC)[4]-mediated inflammation in the kidney (2, 3), joints (4), skin (5, 6), lung (7, 8), and heart (9). A deficiency in Mac-1 is associated with a reduction in complement C3-mediated inflammation in the kidney (10) and skin (11, 12). Both FcγRs and Mac-1 promote neutrophil recruitment and cytotoxicity (13–15). FcγR-induced mast cell secretion of chemokines and cytokines promote neutrophil recruitment and ensuing sequelae (5, 16). FcγRs on neutrophils may also directly contribute to the recruitment to deposited ICs (13). Mac-1 binding of its endothelial ligands, ICAM-1 and 2, promotes neutrophil recruitment in a number of inflammatory models (14). The importance of Mac-1-mediated neutrophil cytotoxicity was defined in a model of thrombohemorrhagic vasculitis by demonstrating the absence of hemorrhage in Mac-1-deficient mice despite normal neutrophil recruitment (12). However, the contribution of neutrophil FcγRs to cytotoxicity in vivo has been difficult to ascertain because genetic deficiency in activating FcγRs leads to a decrease in neutrophil recruitment in all IgG mediated-inflammation models studied to date (3, 8, 17–19). Thus, for FcγRs, it remains unclear whether the ability of these receptors to activate neutrophil cytotoxicity vs their ability to simply bind tissue-deposited ICs to allow cellular recruitment is important in tissue injury in vivo.

The Vav guanine exchange factors link diverse cell surface receptors to activation of Rho GTPases including RhoA, Cdc42, and Rac (20). Studies in primary neutrophils have suggested that Vav proteins 1 and 3, the predominant Vav isoforms in phagocytes, are required for the function of both the β_2 integrins and FcγRs (21, 22). Vav 1,3-deficient (−/−) neutrophils exhibited defects in Mac-1-dependent sustained adhesion to serum-coated plates and the ingestion of serum-opsonized *Escherichia coli*, which were associated with altered Rac1 and RhoA activation (21). Rac proteins 1 and 2, the predominant Rac isoforms in phagocytes, are activated by β_2 integrin ligation (23), but their role in β_2 integrin neutrophil functions remains poorly understood. Vav $1,3^{-/-}$ and Rac $1,2^{-/-}$ neutrophils exhibited severe defects in several FcγR-mediated functions including IgG-mediated phagocytosis, adhesion, and NADPH oxidase-dependent reactive oxygen species generation, suggesting that Vav regulation of Rac is required for these functions (22, 24). Despite the evidence that Vav proteins link FcγRs, Mac-1, and more recently the pattern recognition receptor TLRs (25) to downstream effector responses, the in vivo relevance of these findings is not known.

In this study, we exploited knockout mice and neutrophil reconstitution approaches to examine the contribution of Vav and Rac

*Department of Pathology, Center of Excellence in Vascular Biology, Brigham and Women's Hospital and Harvard Medical School, Boston, MA 02115; and †Faculty of Dentistry, University of Toronto, Toronto, Ontario, Canada

Received for publication June 21, 2007. Accepted for publication February 29, 2008.

The costs of publication of this article were defrayed in part by the payment of page charges. This article must therefore be hereby marked *advertisement* in accordance with 18 U.S.C. Section 1734 solely to indicate this fact.

[1] This work was supported by an American Lung Association Senior Research Fellowship (to A.U.), National Institutes of Health Grants R01 HL065095 and AR050800 (to T.N.M.), and Canadian Institutes of Health Research New Investigator award (to M.G.).

[2] A.U., J.H., and D.M. contributed equally to this work.

[3] Address correspondence and reprint requests to Dr. Tanya N. Mayadas, Brigham and Women's Hospital, Vascular Research Division, 77 Avenue Louis Pasteur, New Research Building 752O, Boston, MA 02115. E-mail address: tmayadas@rics.bwh.harvard.edu

[4] Abbreviations used in this paper: IC, immune complex; RPA, reverse passive Arthus; LSR, local Shwartzman reaction; BMN, none marrow mouse neutrophil; BAL, bronchoalveolar lavage; RT, room temperature; PMN, polymorphonuclear neutrophil.

GTPases in the IgG-mediated reverse passive Arthus (RPA) reaction, a type III hypersensitivity response leading to edema and hemorrhage that requires FcγR but did not depend on Mac-1. In addition, the role of Vav and Rac was evaluated in the local Shwartzman reaction (LSR), a model of thrombohemorrhagic vasculitis characterized by neutrophil accumulation, hemorrhage, fibrin deposition, thrombosis, and elastase release that is dependent on neutrophil Mac-1 and complement C3 deposited within the vessel wall (12, 26). This was coupled with an in vitro assay evaluating the role of Vav and Rac in Mac-1/complement iC3b-dependent neutrophil phagocytosis. We provide evidence that Vav in neutrophils is essential for FcγR/IgG-dependent tissue injury in the skin and lung in vivo at a step downstream of neutrophil recruitment. Rac-deficient mice were also resistant to the skin RPA reaction. The uncoupling of neutrophil recruitment and cytotoxicity demonstrates that FcγR signaling activates neutrophil effector functions that lead to tissue injury in IC disease. In contrast, neither Vav nor Rac were required for Mac-1/complement-dependent neutrophil cytotoxic functions either in vitro or in vivo. These data indicate selectivity for the Vav/Rac pathway in IgG-mediated tissue injury.

Materials and Methods

Mice

C57BL/6J wild-type (WT) mice served as controls for Mac-$1^{-/-}$/C57BL/6 mice (12, 27), and Fcγ chain$^{-/-}$/C57BL/6 mice (Taconic Farms). The sources of C57BL/6J/129Sv Vav$1^{-/-}$, Vav$3^{-/-}$, and Vav $1,3^{-/-}$ mice (28, 29) as well as their WT cohorts are described previously. To minimize the development of strain-dependent genetic differences between lines, we produced WT and single and double Vav isoform-deficient mouse lines from Vav1,3 heterozygous crosses, which were then bred separately for three generations. Previously generated and characterized conditional Rac$1^{-/-}$, Rac$2^{-/-}$, and Rac$1,2^{-/-}$ mice were maintained as a mixed strain population (C57BL/6 and 129Sv) as previously described (30). Homozygous lines were derived from heterozygous crosses as described for Vav$^{-/-}$ mice and were bred separately for five to seven generations. Mice were maintained in a virus- and Ab-free facility at the Eugene Braunwald Research Center animal housing facility at Brigham and Women's Hospital. Mice used for each experiment were between 8 and 20 wk of age and age and sex matched. All experiments in this study were approved by the Harvard Medical School Animal Care and Use Committee.

Neutrophil isolation

For in vitro studies, bone marrow mouse neutrophils (BMN) were isolated as described previously (22). For reconstitution of mice with neutrophils in the RPA reaction, neutrophils were purified from bone marrow as previously described (12), which resulted in a population that was 95% pure as assessed by Wright-Giemsa stains of cytospun samples.

RPA reaction

Skin. For cutaneous RPA reactions, anesthetized age-matched female mice were injected intradermally with rabbit IgG anti-chicken egg albumin Abs (60 μg/30 μl; Cappel), followed immediately thereafter by an i.v. injection of chicken egg OVA (500 μg/mouse; Sigma-Aldrich). The intradermal injection of PBS served as a negative control. In cases where edema was measured, the solution of chicken egg albumin contained 0.15% Evans blue dye (Sigma-Aldrich). The skin was harvested 4 h later.

Reconstitution of neutrophils. For i.v. reconstitution, 7.5×10^6 BMN were given through the tail vein. One hour later, the RPA reaction was initiated as described in the previous section. The skin was harvested 3.5 h later.

Quantification of edema and hemorrhage. Edema was evaluated by measuring the vascular leak of Evans Blue. Harvested skin was incubated with dimethylformamide and Evans blue in the supernatant was quantified by measuring the absorbance at 595 nm. Specific edema formation was measured by subtracting the absorbance in the PBS-injected site from that of the IgG-challenged site in the same mouse. The amount of hemorrhage was assessed 8 h after IC challenge and quantified as described previously (31). The data are reported as the average diameter of the purpuric spot of anti-OVA IgG minus the PBS- injected site of the same mouse.

Histological examination. Skin tissues were harvested 2 or 8 h after IC challenge. Tissues were fixed in 3.5% paraformaldehyde and then paraffin embedded. Six-micrometer sections were deparaffinized and subjected to the chloroacetate esterase reaction to identify neutrophils. Neutrophil infiltration was evaluated by counting extravascular neutrophils within the site of injection as described elsewhere (12).

Lung

The RPA reaction in the lung was induced as described previously (32). Briefly, 800 μg of chicken OVA (Sigma-Aldrich) in 200 μl of PBS was injected via the tail vein in anesthetized mice. One hundred micrograms of rabbit anti-chicken OVA (Cappel) in 100 μl of PBS was instilled into the trachea immediately thereafter. At the end of 4 h, mice were euthanized and bronchoalveolar lavage (BAL) was performed with 1 ml of HBSS plus EDTA. Sham-treated mice were injected intratracheally with buffer alone.

Assessment of lung injury and neutrophils in the BAL. RBC and total white blood cells in the BAL fluid were counted using a hemacytometer. A differential count was obtained on Giemsa-stained cytospun samples. Total BAL neutrophils were determined by multiplying the white blood cell counts by the percentage of neutrophils. Albumin in the BAL was used as an indicator of lung edema and was determined using an ELISA-based method (Bethyl) as previously described (33).

Local Shwartzman reaction

Age-matched Mac-$1^{-/-}$ male mice were i.v. reconstituted with 5×10^6 bone marrow donor neutrophils (Vav WT, Vav$1,3^{-/-}$, Rac WT, or Rac$1,2^{-/-}$) and were subjected to the LSR as described previously (12). In select experiments, skin air pouches were generated and LSR was induced in the pouches (12). The air pouch was lavaged with 3 ml of ice-cold PBS and assayed for elastase release.

Primary granule release assay

An equal number of neutrophils and volume of lavage fluid were added to 24-well plates. Twenty micromolar fluorogenic elastase substrate *N*-methoxysuccinyl-Ala-Ala-Pro-Val-7-amido-4-methylcoumarin (Sigma-Aldrich) was used to measure elastase activity as previously described (12). The fluorescence at 2-min intervals over a 60-min time period was monitored using a plate-based fluorometer with 380 nm excitation and 460 nm emission (Molecular Devices) at 37°C. Samples were then lysed in Triton X-100 to calculate total cellular elastase activity. Elastase activity was proportional to the slope of the increase in fluorescence over time. Percent release of elastase in response to neutrophil adhesion was calculated by dividing elastase activity by the elastase activity detected following lysis of the sample.

Neutrophil binding to and phagocytosis of iC3b-coated sheep RBC

The procedure was originally described to evaluate IgG-mediated phagocytosis (34). A similar approach was adopted but iC3b opsonization was used (35). Briefly, 20% SRBC (Valeant Pharmaceuticals) in PBS (v/v) were opsonized with subagglutinating rabbit IgM anti-sheep RBC (RDI) at room temperature (RT) for 45 min. IgM-coated SRBC were pelleted, washed, and incubated with 20% serum of C5-deficient human serum (Sigma-Aldrich) in PBS with Ca^{2+} and Mg^{2+} for 30 min. After a wash with PBS, IgM-C3 SRBC (C3-RBC) were resuspended in PBS.

To activate β_2 integrins, 1×10^6 bone marrow mouse neutrophils were treated with 1 μg/ml PMA for 15 min at RT in PBS with 1 mM $CaCl_2$ and 0.5 mM $MgCl_2$. RBC were then spun gently, layered on top of the neutrophil pellet, and then respun for an additional 5 min at RT to promote binding. Neutrophils and C3-RBC were then resuspended using a wide bore pipette and incubated at 37C for 1 h. The cell mixture was pelleted and RBC were lysed with H_2O followed by the addition of cold PBS. The cells were repelleted, resuspended in PBS, and visualized under the microscope to assess the total number of internalized RBC in 100 neutrophils.

To measure binding of RBC to neutrophils, RBC were labeled with PKH fluorescence dye as per the manufacturer's instruction (Sigma-Aldrich). PKH-labeled SRBC were then opsonized with IgM and/or IgM and C3. WT and Mac-1 mutant neutrophils were preincubated with allophycocyanin- conjugated anti-Gr-1 Ab (BD Pharmingen) and pretreated with PMA (1 μg/ml) for 15 min at RT, followed by incubation with opsonized or nonopsonized RBC. The mixture was pelleted, resuspended, and incubated on ice for 30 min. The samples were directly analyzed using a flow cytometer and gated for both Gr-1- and PKH-positive signals. The percentage of Gr-1-positive neutrophils that costained with PKH was quantitated.

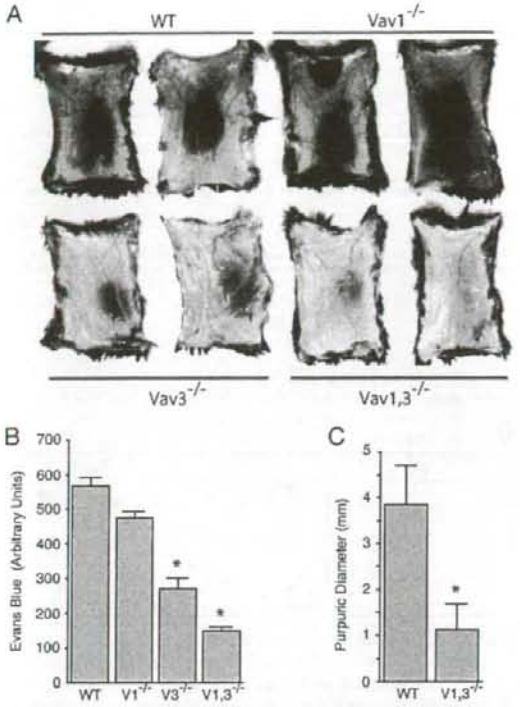

FIGURE 1. The cutaneous RPA reaction. The dorsal skin of WT, Vav 1 ($V1^{-/-}$)-, Vav 3 ($V3^{-/-}$)-, and Vav 1,3 ($V1,3^{-/-}$)-deficient mice were injected intradermally with either anti-OVA (lower back) or as a control (PBS; upper back) followed by an i.v. injection with OVA/0.15% Evans blue. Four hours later, the skin was harvested to examine edema. Evans blue was excluded in evaluation of animals in *C*. *A*, A representative photograph of Evans blue leakage in skins of indicated mice is shown. *B*, The injected sites were excised, Evans blue dye was extracted in dimethyformamide, and absorbance was measured at OD_{595}. Results represent the relative units obtained for the anti-OVA-injected sites minus PBS-injected sites. *, $p < 0.02$ between Vav $3^{-/-}$ or Vav $1,3^{-/-}$ mice and WT animals. $n = 4$/group. *C*, Purpuric diameter as an indicator of hemorrhage was measured 8 h after injection. *, $p < 0.05$; $n = 4$/group. Data are average ± SEM.

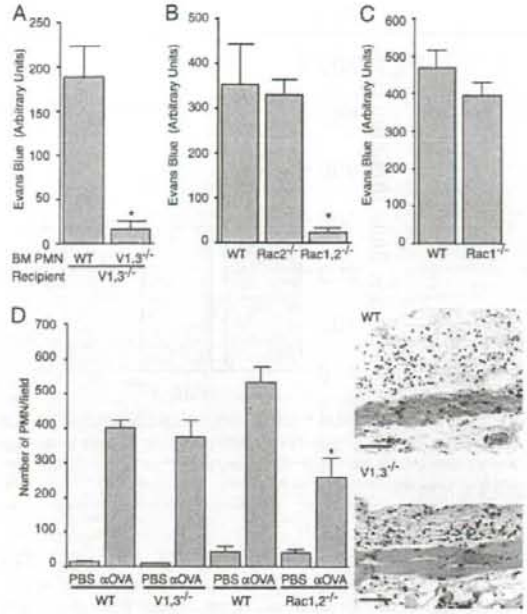

FIGURE 2. Vav on neutrophils, and Rac, are required for edema but not neutrophil recruitment. *A*, The RPA was induced as described in Fig. 1. *A*, The RPA reaction was evaluated in $V1,3^{-/-}$ mice reconstituted i.v. with either WT or $V1,3^{-/-}$ BMN. *, $p < 0.03$; $n = 4$/group. *B*, $Rac2^{-/-}$, $Rac1,2^{-/-}$ mice and (*C*) $Rac1^{-/-}$ and their WT cohorts were subjected to the RPA reaction and Evans blue extravasation was evaluated. *, $p < 0.05$ between Rac $1,2^{-/-}$ and WT. $n = 4$/group in *B* and 8/group in *C*. All data are average ± SEM. *D*, The RPA was induced (with Evans blue excluded) in Vav $1,3^{-/-}$ and Rac $1,2^{-/-}$ mice as indicated. Tissue sections from skin were harvested at 2 h after IC challenge, stained with a specific esterase stain, and the number of neutrophils (PMN) per tissue section was quantitated (*left panel*). Representative H&E-stained tissue sections showing infiltration of neutrophils (stained dark blue) and skin thickness indicative of edema in the skin of WT (*top*) and $V1,3^{-/-}$ (*bottom*) are shown. *, $p < 0.02$; $n = 4$/group. Bar, 140 μm.

Statistical analysis

Quantitative data were represented as mean ± SEM or SD as indicated. Evaluation of statistical significance was performed using a two-tailed unpaired Student's *t* test. Values of $p < 0.05$ were considered statistically significant.

Results

Vav- and Rac-deficient mice fail to develop IgG-mediated edema and hemorrhage in the skin

Vav-deficient mice and their WT cohorts were subjected to the cutaneous RPA reaction to examine the role of Vav in FcγR-dependent functions in vivo. The reaction, induced by an intradermal injection of Ab and i.v. delivery of Ag, is characterized by neutrophil accumulation, edema, and hemorrhage. It is dependent on FcγRs (18) and neutrophil function (36), as confirmed in our studies using Fcγ chain-deficient ($Fc\gamma\ chain^{-/-}$) mice, which lack all activating FcγRs and neutrophil immunodepletion approaches, respectively (data not shown). WT mice and mice deficient in Vav 1, Vav 3, or Vav 1,3 were subjected to the RPA reaction and evaluated for the development of edema, as assessed by the leakage of Evans blue i.v. injected into the mice at the time of Ag delivery. At 4 h after induction of the RPA, Vav $3^{-/-}$ mice exhibited a 50% reduction in Evans blue extravasation in comparison to WT mice, whereas a deficiency in Vav1 alone had no effect. Importantly, Vav $1,3^{-/-}$ mice exhibited minimal edema compared with WT mice (Fig. 1, *A* and *B*). Furthermore, hemorrhage development was significantly reduced in Vav $1,3^{-/-}$ animals compared with WT counterparts (Fig. 1*C*).

To determine whether Vav on neutrophils was responsible for edema, Vav $1,3^{-/-}$ mice were i.v. injected with freshly isolated WT or Vav $1,3^{-/-}$ neutrophils and the reconstituted mice were subjected to the RPA reaction. Adoptive transfer of WT neutrophils into Vav $1,3^{-/-}$ mice resulted in significant edema while transfer of Vav $1,3^{-/-}$ neutrophils resulted in minimal leakage (Fig. 2*A*). These data indicate that Vav 1,3 in neutrophils play a critical role in the development of IC-induced tissue injury. Next, the RPA reaction was evaluated in mice lacking Rac 2 or both Rac 1 and 2 to explore the possibility that the phenotype observed in Vav $1,3^{-/-}$ mice could be explained by a defect in a functional interaction between Vav and Rac proteins in neutrophils in vivo. Mice deficient in Rac 2 or Rac 1 alone developed edema while Rac